AN UPRIGHT POSITIONAL DEVICE AND QUALITY ASSURANCE OF THE TREATMENT PLANNING COMPUTER FOR THE MANTLE FIELD TECHNIQUE

A Thesis
Submitted to the Graduate Faculty of the
Louisiana State University and
Agricultural and Mechanical College
in partial fulfillment of the
requirements for the degree of
Master of Science
in
Nuclear Science
(Medical Radiation Science Option)

by
James M. Pate III
B.S., Louisiana State University, 1991
December, 1996

ACKNOWLEDGMENT

TABLE OF CONTENTS

Page

ACKNOWLEGEMENTS ii

LIST OF FIGURES v

LIST OF TABLES vi

ABSTRACT viii

I. INTRODUCTION 1

II. LITERATURE REVIEW 3

III. DESIGN AND CONSTRUCTION OF MANTLE CHAIR 5

IV. MATERIALS AND METHODS 14

A. Materials

1. Linear Accelerators 14
2. Cerrobend 14
3. Phantom 15
4. Electrometer 15
5. Dosimeter 15
6. Mantle chair 16
7. Computer 16

B. Methods

1. Experimental Set Up 17
2. Leakage Determination 18
3. Output Stability check 20
4. Energy and Dose Determination 20
5. Off-Axis Factor in Air 24
6. Field Size Dependence in Air 25
7. Field Size Dependence in Phantom 26
8. Normalized Peak Scatter Factor 26
9. Percentage Depth Dose 27
10. Tissue Maximum Ratio 27
11. Tray Factor 28
12. Hand Calculations 28

13. Computer Calculations 29
14. Mantle chair 29

V. RESULTS AND DISCUSSION 30

VI. CONCLUSIONS AND RECOMMENDATIONS 64

REFERENCES 67

APPENDIX A: HAND CALCULATIONS 71

ABBREVIATIONS AND ACRONYMS 96

DEFINITIONS 96

VITA 99

LIST OF FIGURES

Figure		Page
1	Photograph of the mantle chair in treatment position front view	8
2	Photograph of the mantle chair in treatment position oblique view	9
3	Front view of the mantle chair	10
4	Side view of the mantle chair	11
5	Attachments for the mantle chair	12
6	Tennis racket style back for the mantle chair	13
7	Water tank setup	19
8	Anterior-posterior chest radiograph of a patient with mediastinal adenopathy showing the position of the tumor mass from a supine position	57
9	Anterior-posterior chest radiograph of a patient with mediastinal adenopathy showing the shift in the tumor mass from a supine to an upright position	58
A.1	Diagram of mantle field test case T13529	72
A.2	Diagram of mantle field test case T12754	77
A.3	Diagram of mantle field test case 13700	83
A.4	Diagram of mantle field test case 13506	89

LIST OF TABLES

Table		Page
1	Summary of the off-axis factor measured at the isocenter for the Clinac 600C in air	31
2	Summary of the off-axis factor measured at the isocenter for the Clinac 4 in air	32
3	Summary of the FSDA values measured at the isocenter for the Clinac 600C in air	33
4	Summary of the FSDA values measured at the isocenter for the Clinac 4 in air	33
5	Summary of the FSDP values measured at the isocenter at d equals d_{max} for the Clinac 600C in phantom	34
6	Summary of the FSDP values measured at the isocenter at d equals d_{max} for the Clinac 4 in phantom	35
7	Summary of the NPSF values for the Clinac 600C	36
8	Summary of the NPSF values for the Clinac 4	36
9	Summary of the PDD values for the Clinac 600C	38
10	Summary of the PDD values for the Clinac 4	40
11	Summary of the TMR values for the Clinac 600C	43
12	Summary of the tray factor values for the Clinac 600C	45
13	Summary of the Tray Factor Values for the Clinac 4	45
14	Comparison of test case T13529 hand calculations and computed data	47

Table Page

15 Comparison of test case T12754 hand calculations and computed data 48

16 Comparison of test case 13700 hand calculations and computed data 49

17 Comparison of test case 13506 hand calculation and computed data 50

18 Comparison of test case T13529 measurements and computed data 52

19 Comparison of test case T12754 measurements and computed data 53

20 Comparison of test case 13700 measurements and computed data 54

21 Comparison of test case 13506 measurements and computed data 55

22 Summary of the FSDP values using the mantle chair for the Clinac 600C in Phantom 59

23 Summary of the NPSF values using the mantle chair for the Clinac 600C ... 59

24 Summary of the PDD values using the mantle chair for the Clinac 600C ... 60

25 Summary of the TMR values using the mantle chair for the Clinac 600C ... 62

A.1 Hand calculation of output factors to CAX and to off-axis points for mantle field technique test case T13529 73

A.2 Hand calculation of output factors to CAX and to off-axis points for mantle field technique test case T12754 78

A.3 Hand calculation of output factors to CAX and to off-axis points for mantle field technique test case 13700 84

A.4 Hand calculation of output factors to CAX and to off-axis points for mantle field technique test case 13506 90

ABSTRACT

The mantle field is a large radiotherapy treatment field technique used to treat patients' with Hodgkin's disease. In clinical studies, it has been shown that some patients with large mediastinal adenopathy show a difference in tumor size width while sitting upright versus the supine/prone position. A smaller size tumor allows for a reduced radiotherapy treatment field size of the lungs and heart than would be if the patient was in a lying position. A reduced treatment field size allows for a lower potential of radiation toxicity to the lungs and heart. The upright positional device therefore enhances the mantle field technique giving the radiation oncologist a better therapeutic ratio with which to treat tumors. The device can also be used to treat lung cancer patients in an upright position who would otherwise suffer discomfort while being treated in the supine position.

INTRODUCTION

Malignant lymphomas are the seventh most common form of cancer in the United States (Holleb, et al, 1991). A common form of treatment for malignant lymphomas is to use radiation therapy. The mantle field technique is used in radiation therapy for irradiation of the supra-diaphragmatic lymph nodes to treat Hodgkin's disease and Non-Hodgkin's lymphomas (Abrahamsen and Host, 1981; Carmel and Kaplan, 1976; Mauch and Buck, 1991; and Page, et al., 1970). The supradiaphragmatic lymph nodes usually treated are the hilar, mediastinal, supraclavicular, axillary, and cervical regions (Wasserman, et al., 1991). The mantle field technique consists of external beam radiation using large field sizes to treat above the diaphragm while minimizing the dose to the critical organs as much as possible. Custom blocking by the mantle technique is to provide blocking to as much uninvolved lung, portions of the heart, and heads of the humerus. Additional shielding to the larynx is normally included in treatment plans when a maximum dose is reached.

Patients at Mary Bird Perkins Cancer Center (MBPCC) are normally treated with anterior-posterior (AP) and posterior-anterior (PA) radiotherapy fields while lying supine/prone on a large Styrofoam support pad seven centimeters high supported by the patient support apparatus (PSA). The head is tilted back on a hard molded Styrofoam support called an "E" headrest. The head is held in place by an aquaplast mask if the treatment field is to include the cervical lymph nodes (Bentel, 1991). An aquaplast

mask is a thermoplastic mesh that is heated in warm water then conformed to the patient's face and allowed to harden.

There are some patients that would be better treated in an upright position instead of lying supine or prone. The reason the patient would receive increased results in treatment in the upright position is because in this position, the mediastinal mass decreases in volume in this new position so that less lung and heart volume is irradiated (Mauch, et al., 1968). With less normal tissue being irradiated, the patient would probably have fewer chances of pulmonary and cardiac complications (Sebaq-Montefiore, et al., 1992). Work done by Marcus et al. (1992) state that, "Approximately 75% of patients with large mediastinal adenopathy (LMA) demonstrate significant differences in the width of the mediastinal disease between the upright and conventional positions" (Leopold, et al, 1989). The conventional positions used are the AP and PA in a supine/prone manner. To decrease the volume of the mediastinal mass, a mantle (radiotherapy) chair can be used to position the patient upright (Karzmark, et al., 1980).

The MBPCC in Baton Rouge, Louisiana, has expressed an interest in a mantle chair. The objectives of this research are:

to design and build a mantle chair so patients can be treated in a reproducible position, and to complete a dosimetry review on the mantle field technique used at MBPCC.

LITERATURE REVIEW

The mantle field is a single radiotherapy treatment field that covers all major lymph nodes above the supra-diaphragmatic and including the neck region while shielding the lungs, heart, and humerus. When a maximum irradiation dosage is reached to the larynx, additional shielding is normally included in treatment plans. The patient is normally treated AP and PA with the mantle field during their radiotherapy treatment. The mantle field was first incorporated at Stanford in 1956 as one of their radiotherapy treatment techniques. Almost all patients with Hodgkin's disease now receive radiotherapy that incorporates the mantle technique. The mantle chair was first designed to treat patients with Hodgkin's disease who showed a tumor size difference between lying supine and sitting upright. The tumor would flatten out while supine but would condense in size while sitting upright. This difference in tumor size is a benefit to a patient so that less healthy tissue is irradiated. Radiation oncologists took advantage of this new anatomical position of the tumor to increased shielding to the critical organ. A shrinking field size technique is used if the tumor responds to treatment. With a smaller tumor treatment area, less healthy lung tissue is exposed to radiation. The benefit of shielding more lung tissue is that the risk of fibrosis and other radiation complications like pericarditis to the patient has been reduced. The mantle chair therefore enhances the mantle field technique giving the radiation oncologist a better therapeutic ratio with which to treat tumors.

Karzmark et al., (1973) developed a versatile radiotherapy treatment chair to treat patients in an upright position. The chair was installed at the end of the treatment

couch and provided x, y and z rotation. The one drawback to the design is that it did not provide isocenter rotation. Isocenter rotation could not occur because a piece of tube steel went up the back of the patient. In treating Hodgkin's disease patients with this chair, only the anterior-posterior treatment field was used.

One of the advantages of using the mantle chair stipulated by Karzmark et al. (1980) were, "Patients with large mediastinal masses, e.g. with Hodgkin's disease, may preferably be treated in the sitting position. The amount of a lung which can be shielded in this position is appreciably greater than when lying down, thus greatly decreasing the morbidity of the treatment."

Boag and Hodt (1971) and Watson et al. (1971) described treatment chairs in published literature. Marcus et al. (1992) described an upright positional device to treat with the mantle field technique. A commercial unit was available from Varian. Varian stop producing their radiotherapy treatment chair in the late nineteen-seventies. The chair that Varian had developed was similar to Karzmark et al. (1973) device in that it fit on the end of the PSA. The reasons given for stopping manufacturing of their device was that the chair was too bulky and heavy for the radiotherapists to handle and the cost of the device. Most radiotherapy cancer centers could not justify the cost for a device that was only going to be used on just a few patients a year. The mantle chair in this thesis only cost approximately $500.00 dollars for materials to build.

DESIGN AND CONSTRUCTION OF MANTLE CHAIR

The mantle chair or the upright positional device is designed for the Clinac 600C* and the Oldelft simulator** to treat patients in a sitting position. The name upright positional device came from treating Non-Hodgkin's lymphomas who had difficulty breathing or experience other discomfort while supine but were not stressed while sitting upright. The reference to mantle chair or upright positional device will be used interchangeably in this thesis.

The design of the upright positional device was to have a way to treat patients while they were sitting with little or no attenuation to the photon beam in the treatment field. The device had to be designed to give a reproducible position throughout their course of treatment. All positional devices reviewed in literature had the drawback of not providing isocenter rotation and only using the AP treatment field. By not having isocenter rotation and the PA field, limited the radiation oncologist from prescribing a better treatment plan when applicable. Isocenter rotation can be used if extended distances are not needed to increase the mantle field size to cover the area to be treated. The PA treatment field was accomplished by using a "tennis racket" back support screen to position the patient instead of a tube steel or x-ray film holder. Figures 3, 4, and 5 present views of the mantle chair.

The positional device is designed to separate into two pieces. The lower half of the positional device falls away from the top half as the upper portion sitting on the

* Varian Associates, Palo Alto, California.
** Oldelft Company, Fairfax, Virginia.

PSA lifts' up. The positional device was finally designed this way to minimize the weight being lifted by the PSA. The upper device weight being lifted during treatment is seventy-five pounds. The upright positional device is designed to go where the tennis racket support normally goes on the PSA.

The elbow and the arm supports are for lifting the arms above the patient's head.

When the arms are above the head, the patient's lymph nodes are shifted from the humerus so the nodes can be treated while shielding the humerus. The elbow supports can be shifted in, out, and the foam pad tilted to a forty-five-degree angle. After doing the literature review, I found that the previous mantle chair designs were not comfortable over extended period of time. To correct this, a padded seat is incorporated in the design. To alleviate arm fatigue, a foam padded elbow support was designed to hold most of the weight. Previously, patients held their arms in the air by grasping a horizontal pole.

The head support utilizes a wooden C-frame with a thermoplastic mesh to hold the patient's head still while being simulated and during radiotherapy treatment. The head support was incorporated instead of a mouth bite block. Some patients have the potential of being mouth breathers instead of breathing through their nasal cavity because of extreme sinus conditions. The thermoplastic mesh allows for easier breathing without the patient experiencing respiration distress. Each support can be raised or lowered in increments of one inch to give each patient a reproducible setup. A car seat belt holds the seated patient against the "tennis racket" back support. The

tennis racket support nylon string was spaced every 1 cm apart. The mesh support was tightened by hand.

The materials used in the construction of the mantle chair consisted of: 1.91 cm (3/4 in.) plywood AB grade, 5.1 X 15.24 cm (2 X 6 in.) fir, 2.54 X 25.4 cm (1 X 10 in.) fir, tennis racket string 15L gauge (1.35 mm), wood glue, and assorted wood screws and fasteners.

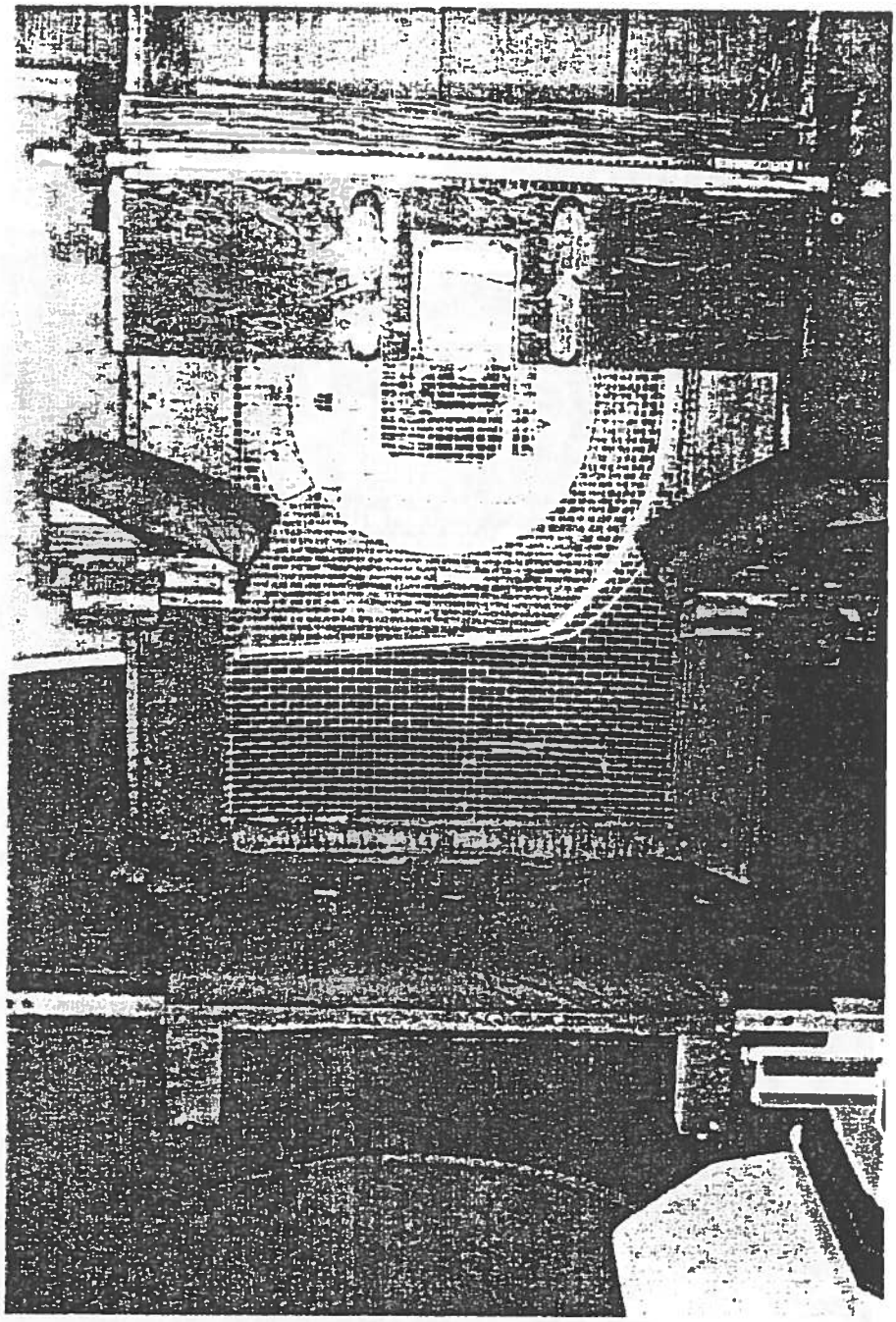

Figure 1. Photograph of mantle chair in treatment position front view.

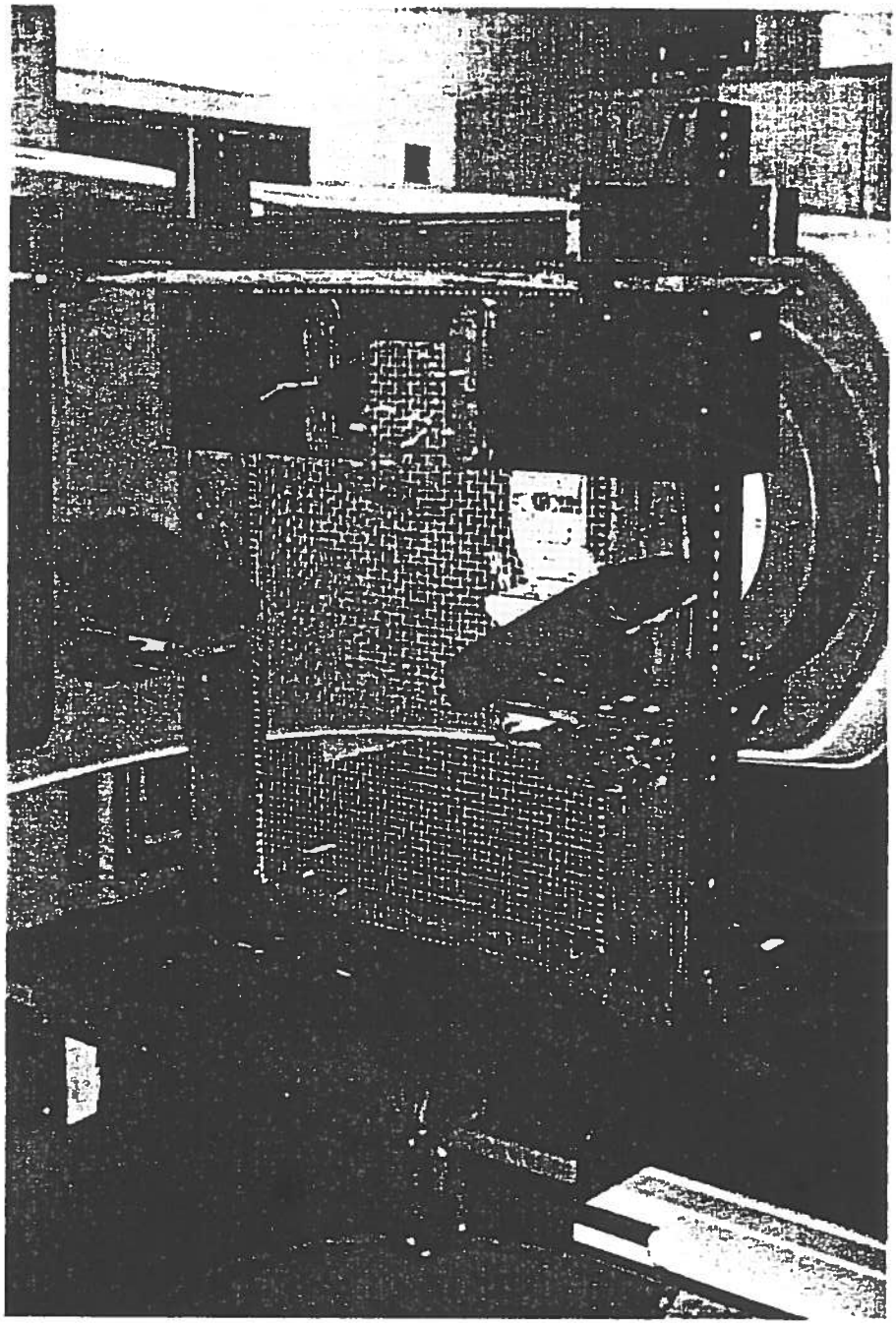

Figure 2. Photograph of the mantel chair in treatment position oblique.

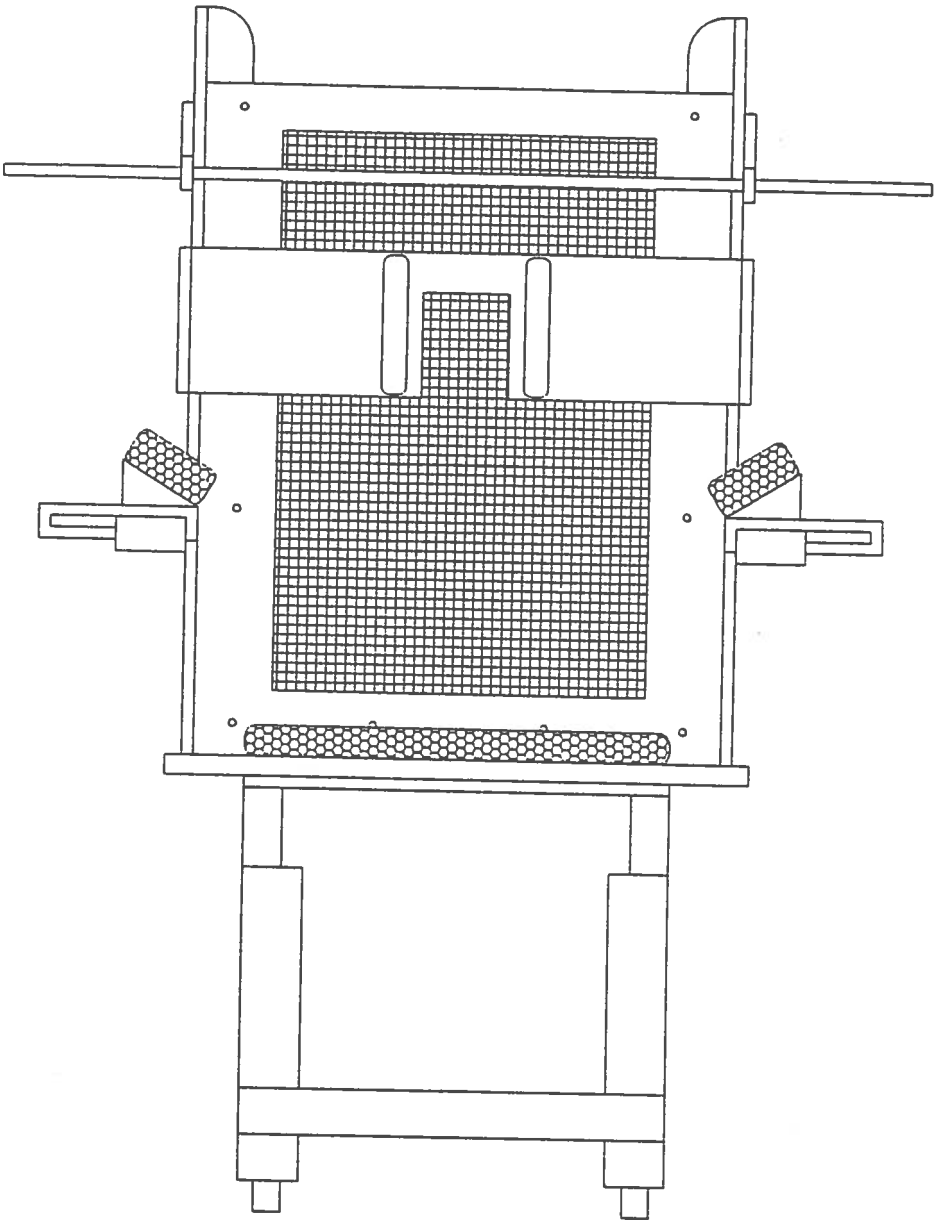

Figure 3. Front view of the mantle chair.

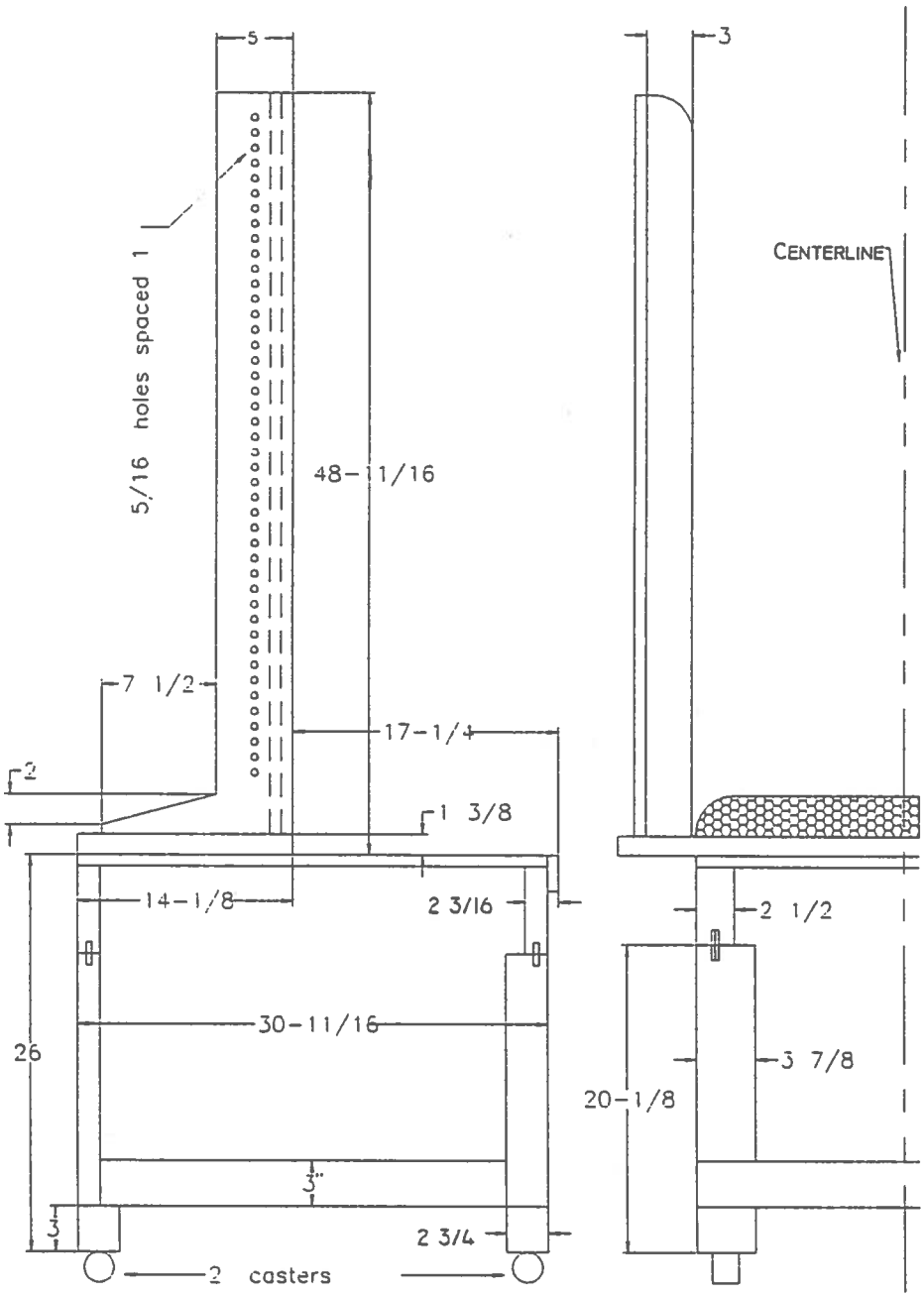

Figure 4. Side view of the mantle chair. All dimensions are in inches. All construction is from 3/4 inch plywood unless noted.

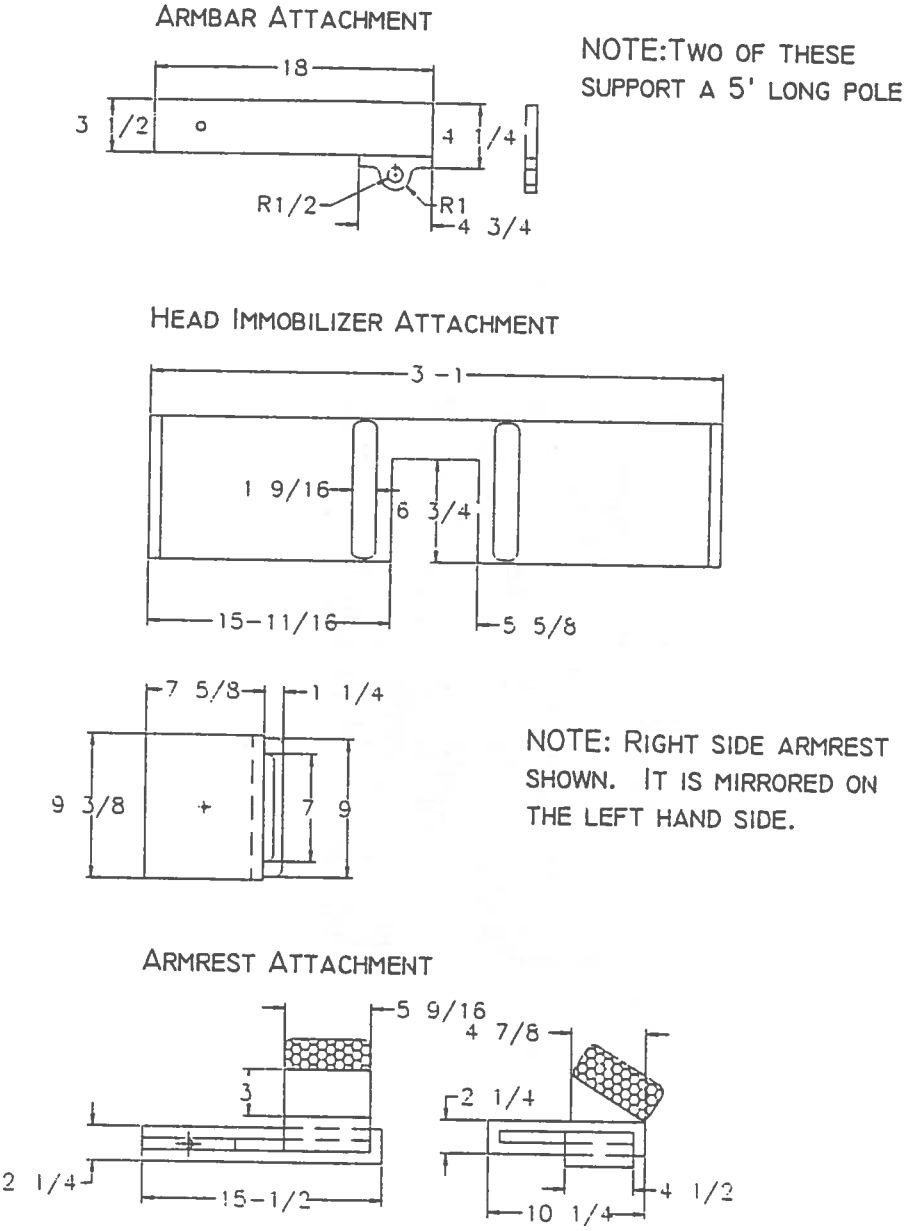

Figure 5. Attachments for the mantle chair. All dimensions are in inches unless noted otherwise.

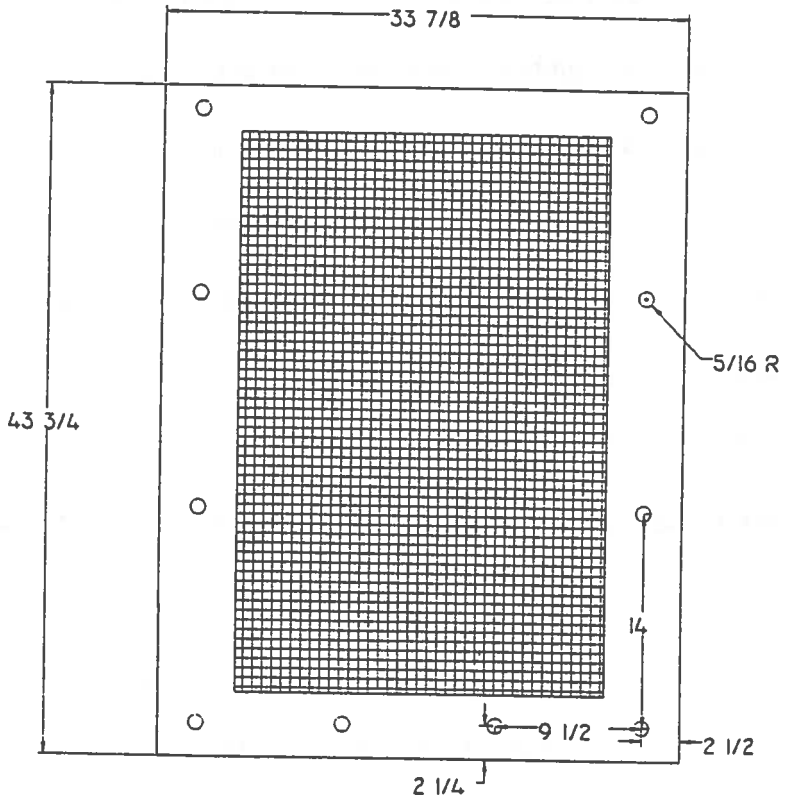

Figure 6. Tennis racket style back support for the mantle chair. All dimensions are in inches.

MATERIALS AND METHODS

A. Materials

1. Linear Accelerators

The materials and equipment in this section are used to do the experiments for this thesis. The Varian Clinac 600C and 4 are standing wave accelerators that incorporates a magnetron tube to produce electrons that are directed into a metal target. The Clinac 600C accelerator produces 6 MV photons and the Clinac 4 produces 4 MV photons. An isocentrically rotationally mounted gantry holds the metal target. The gantry has target to axis distances of 100 cm for the Clinac 600C* and 80 cm for the Clinac 4*. The x-ray beam is collimated by a set collimators usually called "jaws"made of tungsten for the Clinac 600C and depleted uranium for the Clinac 4 . The photon beam is first collimated by a fixed primary set of jaws. The beam is then made more uniform across the treatment field by a flattening filter. The secondary collimators are movable; it defines a rectangular opening through which the photons pass. The field size can be up to 40 cm by 40 cm for Clinac 600c or 32 cm by 32 cm for Clinac 4 at the isocenter. An accessary mount holds customized shielding blocks made out of low temperature melting material called cerrobend**.

2. Cerrobend

The Cerrobend blocking material consisting of 50% bismuth, 26.7% lead, 13.3% tin, and 10.0% cadmium. It is used for making the mantle field blocks that

* Varian Associates, Palo Alto, California.
** Cerrobend is the trade name fo the mixture of metals, it can be purchased from many vendors.

shape the linear accelerator x-ray beam so it serves as a third set of collimators. The x-ray beam is projected as a rectangular field across the body of the patient around the area to be treated. These custom blocks help define the beam to meet treatment protocol. Less healthy tissue is irradiated while treating cancerous cells when using custom blocks.

3. Phantom

A near cubical water tank, constructed with a 1 mm thin window was used to take measurements of dose rates as a function of position. The dimensions of the tank are 40 cm by 42.5 cm by 45.5 cm. An acrylic tube 5 mm thick was used to hold the ionization chamber which in turn was held by a sliding acrylic holder along the top of the phantom. The acrylic tube and holder provided measurement capability in the x, y, and z directions with an incremented scale of 1 cm.

4. Electrometer

The Keithley 614 electrometer has a selectable voltage bias switch for +/-150 or +/-300 volts along with various multiple setting for charge measurements. A Tri-axial cable is connected from the electrometer to the ionization chamber.

5. Dosimeter

This investigation used a NEL-Nylon Chamber Model 2505/2B, serial number 496, Farmer-type cylindrical chamber.

6. Mantle Chair

The mantle chair is an upright positional device used to locate cancer patients in reproducible positions. The device sits on top of the PSA table where the tennis rachet support frame is normally attached.

7. Computer

A Cap-Plan RT110 Radiation Treatment Planning System* computer was used to generate point dose values using irregular fields for comparison to measured data and hand calculations. The Cap-Plan RT110 algorithm uses scatter-maximum ratios to calculate doses within an irregular field. A mantle field is considered an irregular field because it is not rectangular in shape. See figure A.4 in Appendix A: Hand Calculations for a standard looking mantle field.

* Cap-Plan RT110 is no longer available.

B. METHODS

1. Experimental Set Up

Three experiments were accomplished to support this thesis. The first one to check the dosimetric data used at MBPCC, like Off Axis Factor in Air (OAF), Field Size Dependence in Air (FSDA), Field Size Dependence in Phantom (FSDP), Normalized Peak Scatter Factor (NPSF), Percentage Depth Dose (PDD), Tissue Maximum Ratio (TMR), and Tray Factor (TF). The reason to check and confirm the data already established in reference dosimetry books at MBPCC is, that this reference data will be used in hand calculations in appendix A to check the Cap-Plan computer calculations for mantle field irradiation.

The second experiment was to check the effect the mantle chair on the photon beam so that correction factor could be applied if necessary in calculating monitor units for treatment planning. The data were taken with the gantry rotated 90 degrees. The acrylic water phantom was raised by placing particle board underneath the phantom on top of the sitting area of the mantle chair.

The third experiment was to take past patient cases that used mantle field blocking and to compare measured output doses in a water tank to the Cap-Plan computer generated treatment plans. The water tank has a 1 mm thin acrylic window which was turned towards the linear accelerator beam. The water tank used is capable of being moved in three dimensions in the x, y, and z directions. Looking at a front view of a patient, the x direction was the height, the y direction was the lateral shift, and the z direction was the depth. See figure 7 to see the water tank set-up with the

linear accelerator. To measure the dose rate at different points, a reference output factor was first measured three times and averaged using 100 machine uints, 10 x 10 cm^2 FS, SSD of 80 cm for the Clinac 4 and 100 cm for the Clinac 600C, and TPC corrected. The chamber was then placed at points being used in the Cap-Plan computer treatment plans. Three measurements were made at these points and were averaged and TPC corrected. The average measurement were then divided by the reference output factor and corrected by the contancy reading. What was actually used in the test cases from past patient cases was the mantle field blocking design from the x-ray port film only.

2. Leakage Determination

The current leakage measurement was performed to determine if the Keithly electrometer or the Farmer-type cylindrical ion chamber were or were not working appropriately. The leakage from the cylindrical ion chamber was measured with the Keithly 614 electrometer and a stopwatch. The stopwatch was started when the electrometer displayed 0.001 constantly. A minimum of 15 minutes must have passed before reading electrometer number displayed that was not bouncing between zero and 0.001. The initial reading, 0.001, was then subtracted from all subsequent indications numbers. This corrected number was then multiplied by the electrometer correction factor for that particular electrometer. Division by this number was then divided by the elapse time yields the current in Amperes.

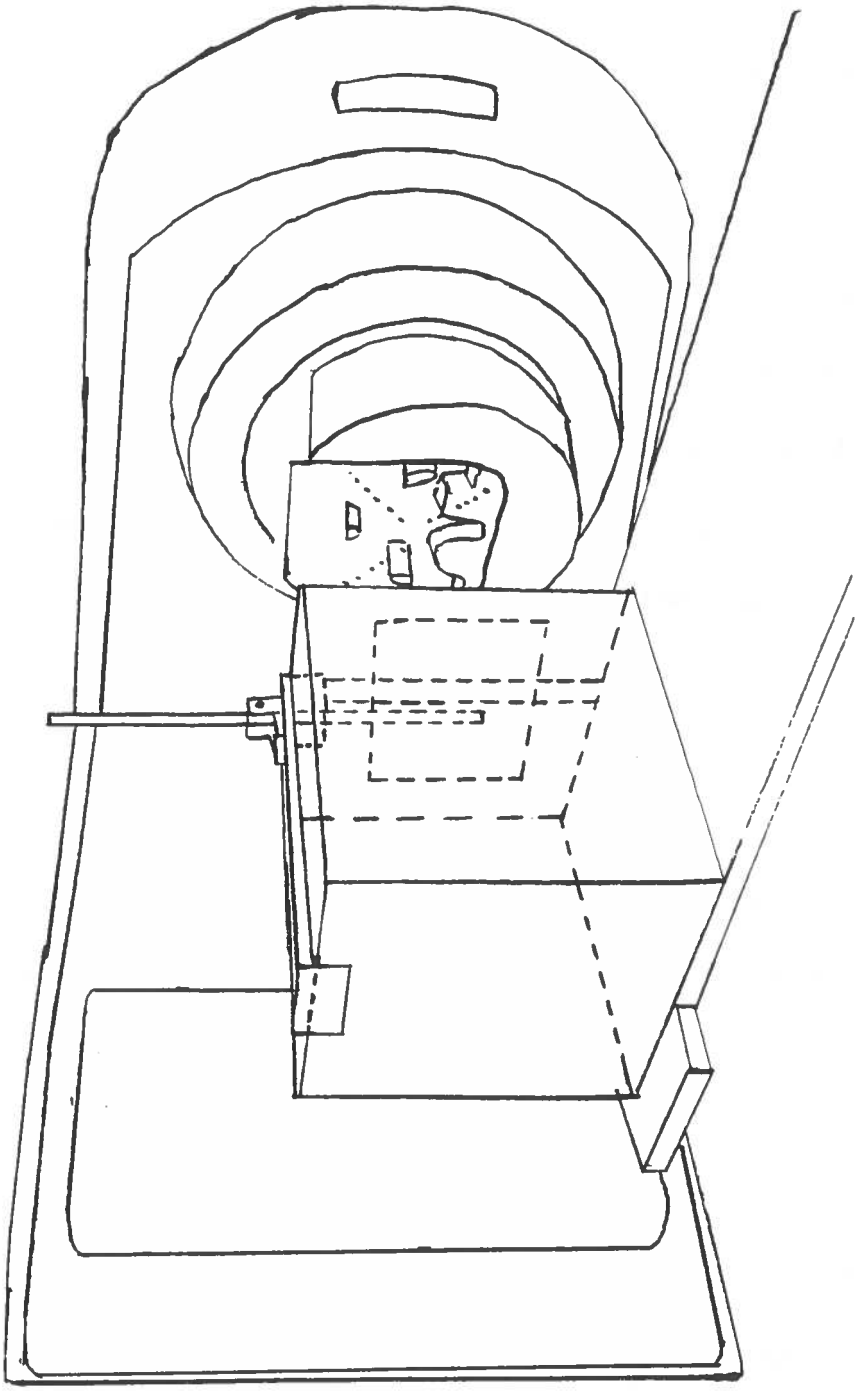

Figure 7. Water tank setup.

3. Output Stability Check

The output stability check was done in the same manner for morning quality assurance check out. The linear accelerator goes through its time delay and warming up by running 999 machine units. The gantry was rotated to 90 degrees with the cylindrical ion chamber held in place by a special attachment. The special attachment places the ion chamber at a distance equal to (SSD + dmax) for that particular energy and machine. One hundred monitor units were then run with the electrometer measuring the reading. One monitor unit is equal to one rad for a field size of 10 X 10 cm^2. Three successive measured readings were then averaged. The average reading was then corrected for temperature (T) and pressure (P) found in equation 1:

$$TPC = \frac{T + 273.15}{295.15} * \frac{760}{P} \quad (1)$$

Where T is temperature in °C and P is pressure in mm Hg.

4. Energy and Dose Determination

Energy and dose determinations were performed to measure output. This was important for two reasons in that this assured that the experiments were performed with linear accelerators within the acceptable standards. If the linear accelerators would have not been calibrated for one rad/mu for a 10 X 10 cm^2 field size, but were within acceptable standards, this would have led to an additional correction factor when comparing measured output dose to computer generated data. The quality assurance procedure used to determine that the linear accelerator output was one rad/MU for a 10 X 10 cm^2 field size was performed by TG-21 Protocol (AAPM, 1983). The following

equation (2) is used for determining the output of the accelerator in terms of dose rate, $\dot{D}$, in rads/monitor unit.

$$\dot{D}\ (rads/mu) = M * TPC * N_x * N_{gas}/(N_x * A_{ion}) * \left(\frac{L}{\rho}\right)_{air}^{med} * P_{wall} * P_{repl} * P_{cap} * P_{ion} * \left(\frac{\mu}{\rho}\right)_{med}^{H_2O} * ECF * \left(\frac{\mu}{\rho}\right)_{H_2O}^{muscle} * (DDF)^{-1} * (mu + e)^{-1} \quad (2)$$

Where in equation two $\dot{D}$ is the dose rate, $\overline{M}$ is the average electrometer reading, TPC is the temperature and pressure correction factor explained by equation 1, N_x is the ^{60}Co exposure calibration factor (R/C) of the chamber volume and build up cap. The term $N_{gas}/(N_x * A_{ion})$ represents the calibration of the volume of gas in a particular chamber in terms of absorbed dose per unit of exposure. The value for this term is 8.42 (cGy/R) and was obtained from a table in Khans' (1994) "The Physics of Radiation Therapy." The $\left(\frac{L}{\rho}\right)_{air}^{med}$ is the ratio of the restricted mass stopping power of the phantom material to that of air. The P_{wall} is the correction factor for the difference in the material of the chamber wall and the phantom. The P_{wall} is found from equation 3:

$$P_{wall} = \frac{(\alpha \left(\frac{\overline{L}}{\rho}\right)_{air}^{wall} \left(\frac{\overline{\mu}_{EN}}{\rho}\right)_{wall}^{med} + (1 - \alpha)\left(\frac{\overline{L}}{\rho}\right)_{air}^{med}}{\left(\frac{\overline{L}}{\rho}\right)_{air}^{med}} \quad (3)$$

In equation 3 alpha (α) is the fraction of the amount of cavity air ionization in the ion chamber due from electrons generated in the chamber wall and (1 - :) from the medium. The $\left(\frac{\overline{\mu}_{EN}}{\rho}\right)^{med}_{wall}$ term is the ratio of the mean mass energy absorption coefficient of medium to the wall. The $\left(\frac{\overline{L}}{\rho}\right)^{med}_{air}$ is the average restricted mass collisional stopping power of electrons of the medium to that of air.

Continuing defining the terms in equation 2. The term P_{repl} is the correction factor which accounts for perturbations of photon fluence at point P when the medium replaces the chamber. The P_{repl} is found from published values. The P_{cap} is the correction factor that takes into account attenuation of the cap. The P_{cap} is found from published values. The P_{ion} is the correction factor for ion recombination loss in the electrometer and is measured at two different voltages, usually at -150 V and -300 V. P_{ion} was measured by setting the electrometer voltage to -150 V or -300 V, with three readings averaged and TPC corrected, running 100 machine units, SSD at 100 cm for Clinac 600C or 80 cm for the Clinac 4, 10 X 10 cm^2 F.S., at a depth of 5 cm. Then the -300 V ($\overline{M}^{*}_{-300V}$) measured corrected reading is divided by the -150 V ($\overline{M}^{*}_{-150V}$) measured corrected reading.

$$P_{ion} = \frac{\overline{M}^{*}_{-300V}}{\overline{M}^{*}_{-150V}} \qquad (4)$$

Continuing defining the terms in equation 2. The $\left(\frac{\mu}{\rho}\right)^{H_2O}_{med}$ term being the correction factor of the ratios of the mean mass energy absorption coefficients of water

to the medium. The ECF is the electrometer correction factor in units of coulombs per unit reading. The $\left(\frac{\mu}{\rho}\right)_{H_2O}^{muscle}$ term being the correction factor of the ratios of the mean mass energy absorption coefficients of muscle tissue to that of water. The $(DDF)^{-1}$ is the depth dose fraction for five centimeter depths. The $(mu + e)^{-1}$ are the monitor units used in calibration plus the end effect. The end effect, e, is obtained from the equation 5:

$$e = \frac{100 * (M_{4*25} - \overline{M}_{100})}{(4 * \overline{M}_{100}) - M_{4*25}} \qquad (5)$$

In equation 5, the term M_{4*25} means the measured reading is taken in increments of 25 monitor units four times without resetting the electrometer. $\overline{M}_{100}$ is the average electrometer reading using 100 monitor units.

The ionization ratio (IR) is used to determine the nominal accelerating potential (NAP) from a graph of IR versus NAP. NAP is used to characterize a x-ray energy being look at. The measurement is made from the source to target axis distance (TAD) using two different depth thicknesses. The target being the ion chamber. The Clinac 600C has a TAD of 100 cm. The Clinac 4 has a TAD of 80 cm. The two different depth thicknesses use a ratio of a tissue maximum ratio (TMR) of 20 cm and 10 cm. The field size is 10 x 10 cm^2 at the placement of the ion chamber. The following equation (6) is used to find IR.

$$Ionization\ Ratio = \frac{TMR_{(20)}}{TMR_{(10)}} \qquad (6)$$

5. Off-Axis Factor in Air

The off-axis factors in air measurements were taken for the Clinac 600C and the Clinac 4. Off-axis factors take into account the cross beam profile which is dose variation across the field of that particular linear accelerator. The measurements were taken in air with a Farmer type cylindrical ion chamber with the appropriate buildup cap for the 6 MV and 4 MV energies. The ion chamber was placed on top of a tennis racket support screen. The chamber was moved every two centimeters starting from the central axis (CAX) for measurements. The field size for the Clinac 600C was 40 x 40 cm with measurements taken to 18 cm distance. The Clinac 4 field size was 30 x 30 cm with measurements made to 14 cm distance. The cross beam profiles were measured in the plus or minus x and y direction. The three measurements taken at the CAX were averaged ($\overline{M}$) and then temperature and pressure corrected (TPC). All off axis points have three measurements taken, averaged, and corrected for TPC. The off axis points were then normalized by being divided by the corrected central axis (CAX) measurement. The Off Axis Factor is used to correct the dose rate at any point away from the central axis (Cundiff, et al., 1973; Hoppe, 1985; Khan, 1994). The equation for OAF_{air} can be written as :

$$OAF_{air} = \frac{\overline{M}_{(p,\,FS_{40x40})}}{\overline{M}_{(CAX,\,FS_{40x40})}} \qquad (7)$$

Where $\overline{M}$ is the TPC corrected average electrometer reading. Point "p" is the off axis distance. The 40 x 40 (for Clinac 600C) or the 30 x 30 (for Clinac 4) is the collimator field size (FS_{COLL}). CAX is the central axis.

6. Field Size Dependence in Air

Field size dependence in air (FSDA) was determined for both the Clinac 600C and the Clinac 4. The Clinac 600C FSDA measurements were done for field sizes 6 x 6, 8 x 8, 10 x 10, 15 x 15, 20 x 20, 30 x 30, and 40 x 40 cm^2. A 6 MV build-up cap was used on the ion chamber. The SSD will be 98.5 cm to the top of the build-up cap at the CAX. Three measurements were taken for each field size, averaged, and corrected for TPC. All field sizes (FS) were normalized to the 10 x 10 cm^2 FS.

The Clinac 4 FSDA measurements were made for field sizes 5 x 5, 6 x 6, 8 x 8, 10 x 10, 15 x 15, 20 x 20, 30 x 30 cm^2. A 4 MV build-up cap was used on the ion chamber. The SSD was 78.8 cm to the top of the build-up cap at the CAX. Three measurements were taken to determine the average value $\overline{M}$ for each field size, averaged, and corrected for TPC. All field sizes were normalized to the 10 x 10 cm^2 FS. Equation 8 defines FSDA as:

$$FSDA = \frac{\overline{M}_{(FS_{coll})\,air}}{\overline{M}_{(FS_{10x10})\,air}} \qquad (8)$$

7. Field Size Dependence in Phantom

Field size dependence in phantom was determined for the Clinac 600C and the Clinac 4. The Clinac 600C FSDP measurements were for field sizes 6 x 6, 8 x 8, 10 x 10, 15 x 15, 20 x 20, 30 x 30, and 40 x 40 cm^2. The isocenter is 100 cm to the center of the chamber and 98.5 cm SSD to the side of the acrylic phantom at the CAX. Three measurements $\overline{M}$ were taken for each field size, averaged, and corrected for TPC. All field sizes were normalized to the 10 x 10 cm^2 FS.

The Clinac 4 FSDP was determined for field sizes 5 x 5, 6 x 6, 8 x 8, 10 x 10, 15 x 15, 20 x 20, 30 x 30 cm^2. The isocenter is 80 cm to the center of the chamber and 78.8 cm SSD to the side of the acrylic phantom at the CAX. Three measurements were taken to determine the average value $\overline{M}$ for each field size, averaged, and corrected for TPC. All field sizes were normalized to the 10 x 10 cm^2 FS. The following equation defines FSDP as:

$$FSDP = \frac{\overline{M}_{(d_{max},\, FS_{coll})\,phantom}}{\overline{M}_{(d_{max},\, FS_{10X10})\,phantom}} \qquad (9)$$

8. Normalized Peak Scatter Factor

The normalized peak scatter factor (NPSF) is derived from the FSDA and FSDP measured data. The following equation is used to obtain the NPSF:

$$NPSF = \frac{FSDP_{(d_{max},\, FS)}}{FSDA_{(d_{max},\, FS)}} \qquad (10)$$

9. Percentage Depth Dose

The percentage depth dose (PDD) was measured for the Clinac 600C and the Clinac 4. The Clinac 600C PDD measurements were made for field sizes 5 x 5, 8 x 8, 10 x 10, 15 x 15, 20 x 20, 30 x 30, and 40 x 40 cm^2. The SSD is 100 cm to the surface of the acrylic phantom at the CAX. Each field size at dmax had three measurements averaged, and corrected for TPC. All other depths for that particular field sizes were normalized to dmax. The depths measured were 1.5, 5.0, 10.0, 15.0, 20.0 cm^2.

The Clinac 4 PDD measurements were made for field sizes 5 x 5, 6 x 6, 8 x 8, 10 x 10, 15 x 15, 20 x 20, and 30 x 30 cm^2. The SSD is 80 cm to the surface of the acrylic phantom at the CAX. Each field size at dmax had three measurements to determine the average value averaged, and corrected for TPC. All other depths for that particular field sizes' were normalized to that particular field size dmax. The depths (d) measured were 1.2, 5.0, 10.0, 15.0, and 20.0 cm. The following equation is used to calculate percentage depth dose:

$$PDD = \frac{DOSE_{(d,\, FS_{surface})}}{DOSE_{(d_{max},\, FS_{surface})}} \qquad (11)$$

10. Tissue Maximum Ratio

The tissue maximum ratio measurements were made on the Clinac 600C for field sizes 5 x 5, 8 x 8, 10 x 10, 15 x 15, 20 x 20, 30 x 30, 40 x 40 cm. The cylindrical Farmer type ion chamber was set at the isocenter of the machine so the SSD will vary

from depth to depth. The SSD to the surface of the acrylic phantom will be 100 cm minuses the depth being measured. Each field size will have three measurements to determine the average value $\overline{M}$ taken, averaged, and corrected for TPC. The measurements at dmax (1.5 cm) will be normalized to one. All other depths for that particular field sizes will be normalized to dmax. The depths (d) measured were 1.5, 5.0, 10.0, 15.0, and 20.0 cm. The term FS_p is the field size at the point of measurement. Equation 12 defines the tissue maximum ratio as:

$$TMR = \frac{DOSE_{(d,\,FS_p)}}{DOSE_{(d_{max},\,FS_p)}} \qquad (12)$$

Where FS_p is the field size at point $_p$.

11. Tray Factor

The tray factor determination in this study is to measure the transmission of the photon beam using an acrylic tray with Cerrobend blocking. Using 100 MU, an average of three readings, temperature and pressure corrected were taken with and without an acrylic tray with Cerrobend blocking in place. The average readings $\overline{M}$ were then normalized to the open readings without an acrylic tray with Cerrobend blocking.

12. Hand Calculations

Hand calculations were done for four mantle field test cases. The Clinac 600C and the Clinac 4 each will have two mantle field test cases done. The results of each test case will be compared to Cap-Plan computer generated data. The method used to

judge the effective field size for hand calculations was Khan's Approximation Method [25]. Equation 13 was used to get the hand calculation results.

$$DOSE = (100\ MU \times FSDA_{coll} \times NPSF(EffFS_d) \times \%DD \times TF \times OAF \times ISQ \times MF) \quad (13)$$

Refer to the appendix table A: Hand Calculation for the actual hand calculations along with the diagrams for each test case.

13. Computer Calculations

Computer calculations were done for four mantle field test cases. The Clinac 600C and the Clinac 4 each have two mantle field test cases done. The results of each test case were compared to measured output data. Past patients' cases were used to get the mantle field Cerrobend blocking design to be used in getting measured data, computer generated data from the Capintec computer, and hand calculations.

14. Mantle Chair

The mantle chair was tested and used on the Clinac 600C and Oldeft simulator. The tests done on the Clinac 600C were spot-checking dosimetric values used at MBPCC against measured values. The readings were taken at a ninety-degree gantry position with the beam PA to the rear of the mantle chair. Refer to photograph on page eight.

RESULTS AND DISCUSSION

Using the American Association of Physicists in Medicine (AAPM) TG-21 protocol, the dose rate for the Clinac 600C was found to be 1.000 rad/MU for a 10 X 10 cm^2 FS at SSD and dmax, after taking into account the constancy reading. The dose rate for the Clinac 4 was found to be 1.001 rad/MU, after taking into account the constancy reading. Doing this also insured that the phantom and the chamber used were suitable for taken measurements.

The off-axis factor in air measurements for the Clinac 600C and Clinac 4 were found to be within plus or minus two percent of the Mary Bird Perkins Cancer Center (MBPCC) dosimetric values used for hand calculations. Tables one and two on the following two pages show the results of the measurements taken compared to the dosimetric values used.

The plus or minus two percent criteria was chosen for the following reasons. MBPCC utilizes the plus or minus two percent to stay within AAPM guidelines. Faiz M. Khan (1994), Gerald J. Kutcher, et al. (April 1994), and J. Van Dyk, et al (1993) stipulates the plus or minus two percent for full calibration for quality assurance. The plus or minus two percent criteria takes into account that measured data compared to previously taken data will have some deviations from the original data because of equipment and human error. The equipment error can come from linear accelerators, ion chambers, and electrometers being out of adjustment or calibration. Human error normally comes from incorrect positioning of the ion chamber, SSD, field size, or monitor units used.

Table 1. Summary of the off-axis factor values measured at the isocenter for the Clinac 600C in air.

OAD (CM)	OAF Measured	OAF Used at MBPCC	Ratio= Measured/Used
0	1.000	1.00	1.00
2	1.007	1.02	0.99
4	1.018	1.03	0.99
6	1.024	1.04	0.99
7	1.026	1.04	0.99
8	1.028	1.04	0.99
9	1.029	1.05	0.98
10	1.032	1.05	0.98
11	1.034	1.05	0.99
12	1.037	1.05	0.99
13	1.040	1.05	0.99
14	1.043	1.06	0.98
15	1.046	1.06	0.99
16	1.048	1.06	0.99
17	1.050	1.05	1.00
18	1.050	1.05	1.00

Off-axis factor in air (OAF) is averaged in the X_1 , X_2 , Y_1 , Y_2 directions.

Table 2. Summary of the off-axis factor measured at the isocenter for the Clinac 4 in air.

OAD (CM)	OAF Measured	OAF Used at MBPCC	Ratio= Measured/Used
0	1.00	1.00	1.00
2	1.04	1.04	1.00
4	1.09	1.08	1.01
6	1.11	1.11	1.00
8	1.13	1.12	1.01
10	1.14	1.14	1.00
12	1.16	1.15	1.01
14	1.14	1.13	1.01

Off-axis factor in air (OAF) is averaged in the X_1 , X_2 , Y_1 , Y_2 directions.

The field size dependency in air measurements for the Clinac 600C and Clinac 4 were found to be within plus or minus one percent of the MBPCC dosimetric values used. Tables three and four show the results of the measurements taken to the MBPCC dosimetric values used.

Table 3. Summary of the FSDA values measured at the isocenter for Clinac 600C in air.

FS_{coll}	FSDA	FSDA Used at MBPCC	Ratio= Measured/Used
6 x 6	0.981	0.981	1.000
8 x 8	0.991	0.992	0.999
10 x 10	1.000	1.000	1.000
15 x 15	1.012	1.013	0.999
20 x 20	1.020	1.021	0.999
30 x 30	1.029	1.029	1.000
40 x 40	1.031	1.034	0.997

Table 4. Summary of the FSDA values measured at the isocenter for Clinac 4 in air.

FS_{coll}	FSDA	FSDA Used at MBPCC	Ratio= Measured/Used
5 x 5	0.974	0.975	0.999
6 x 6	0.980	0.982	0.998
8 x 8	0.991	0.992	0.999
10 x 10	1.000	1.000	1.000
15 x 15	1.013	1.013	1.000
20 x 20	1.022	1.022	1.000
30 x 30	1.026	1.032	0.994

The field size dependency in phantom measurements for the Clinac 600C and Clinac 4 were found to be within plus or minus one percent of the MBPCC dosimetric values used. Tables five and six on the following page show the results of the measurements compared to the values used.

Table 5. Summary of the FSDP values measured at the isocenter at d equals d_{max} for Clinac 600C in phantom.

FS_{coll}	FSDP	FSDP Used at MBPCC	Ratio= Measured/Used
6 x 6	0.956	0.950	1.006
8 x 8	0.982	0.980	1.002
10 x 10	1.000	1.000	1.000
15 x 15	1.035	1.035	1.000
20 x 20	1.058	1.058	1.000
30 x 30	1.086	1.086	0.999
40 x 40	1.103	1.104	0.999

The SCD is 100 cm to the center of the chamber.

Table 6. Summary of the FSDP values measured at the isocenter at d equals d_{max} for Clinac 4 in phantom.

FS_{coll}	FSDP	FSDP Used at MBPCC	Ratio= Measured/Used
5 x 5	0.953	0.958	0.995
6 x 6	0.966	0.968	0.997
8 x 8	0.983	0.985	0.998
10 x 10	1.000	1.000	1.000
15 x 15	1.029	1.027	1.003
20 x 20	1.051	1.046	1.004
30 x 30	1.069	1.072	0.997

The SCD is 80cm to the center of the chamber.

The normalized peak scatter factor is derived from the FSDP and FSDA. The NPSF for the Clinac 600C and Clinac 4 were found to be within plus or minus one percent of the MBPCC dosimetric values used. Tables seven and eight show the results of the measurements taken compared to the MBPCC dosimetric values used. The equation 10 is used to get NPSF.

Table 7. Summary of the NPSF values for the Clinac 600C.

FS_{coll}	FSDP	FSDA	NPSF*	NPSF Used at MBPCC	Ratio= Measured/Used
6 x 6	0.970	0.981	0.989	0.988	1.001
8 x 8	0.987	0.992	0.995	0.994	1.001
10 x 10	1.000	1.000	1.000	1.000	1.000
15 x 15	1.023	1.013	1.009	1.012	0.997
20 x 20	1.041	1.019	1.022	1.020	1.002
30 x 30	1.061	1.029	1.031	1.030	1.001
40 x 40	1.068	1.029	1.038	1.037	1.001

* Note: NPSF= FSDP/FSDA

Table 8. Summary of the NPSF values for the Clinac 4.

FS_{coll}	FSDP	FSDA	NPSF*	NPSF Used at MBPCC	Ratio= Measured/Used
5 x 5	0.953	0.974	0.978	0.979	0.999
6 x 6	0.966	0.980	0.986	0.983	1.003
8 x 8	0.983	0.991	0.992	0.992	1.000
10 x 10	1.000	1.000	1.000	1.000	1.000
15 x 15	1.029	1.013	1.016	1.015	1.001
20 x 20	1.051	1.022	1.028	1.021	1.007
30 x 30	1.069	1.026	1.042	1.032	1.009

* Note: NPSF= FSDP/FSDA

The percentage depth dose measurements for the Clinac 600C and Clinac 4 were found to be within plus or minus two percent of the MBPCC dosimetric values used. Tables 9 through 12 on the following pages compare of the measurements from this thesis to the standard MBPCC dosimetric values.

Table 9. Summary of the PDD values for the Clinac 600C.

Depth (cm)	FS_{coll} (cm)	Average readings x TPC	PDD	PDD Used at MBPCC	Ratio= Measured/Used
1.5 cm	5 x 5	2.191	1.000	1.000	1.000
1.5 cm	8 x 8	2.254	1.000	1.000	1.000
1.5 cm	10 x 10	2.285	1.000	1.000	1.000
1.5 cm	15 x 15	2.341	1.000	1.000	1.000
1.5 cm	20 x 20	2.380	1.000	1.000	1.000
1.5 cm	30 x 30	2.430	1.000	1.000	1.000
1.5 cm	40 x 40	2.445	1.000	1.000	1.000
5 cm	5 x 5	1.836	0.838	0.843	0.994
5 cm	8 x 8	1.923	0.853	0.853	1.000
5 cm	10 x 10	1.960	0.858	0.865	0.992
5 cm	15 x 15	2.025	0.865	0.872	0.992
5 cm	20 x 20	2.070	0.869	0.876	0.992
5 cm	30 x 30	2.126	0.875	0.881	0.993
5 cm	40 x 40	2.146	0.877	0.884	0.992
10 cm	5 x 5	1.361	0.621	0.626	0.992
10 cm	8 x 8	1.459	0.647	0.654	0.989
10 cm	10 x 10	1.508	0.659	0.667	0.988
10 cm	15 x 15	1.590	0.679	0.688	0.987
10 cm	20 x 20	1.642	0.689	0.698	0.987
10 cm	30 x 30	1.709	0.703	0.711	0.989
10 cm	40 x 40	1.736	0.710	0.716	0.992

Continuing Table 9. Summary of the PDD values for the Clinac 600C.

Depth (cm)	FS_{coll} (cm)	Average readings x TPC	PDD	PDD Used at MBPCC	Ratio= Measured/Used
1.5 cm	5 x 5	2.194	1.000	1.000	1.000
1.5 cm	8 x 8	2.259	1.000	1.000	1.000
1.5 cm	10 x 10	2.289	1.000	1.000	1.000
1.5 cm	15 x 15	2.346	1.000	1.000	1.000
1.5 cm	20 x 20	2.386	1.000	1.000	1.000
1.5 cm	30 x 30	2.434	1.000	1.000	1.000
1.5 cm	40 x 40	2.450	1.000	1.000	1.000
15 cm	5 x 5	1.026	0.467	0.466	1.003
15 cm	8 x 8	1.119	0.496	0.493	1.006
15 cm	10 x 10	1.167	0.509	0.507	1.006
15 cm	15 x 15	1.253	0.534	0.531	1.006
15 cm	20 x 20	1.309	0.549	0.547	1.003
15 cm	30 x 30	1.378	0.566	0.566	1.000
15 cm	40 x 40	1.405	0.573	0.576	0.996
20 cm	5 x 5	0.758	0.345	0.340	1.016
20 cm	8 x 8	0.838	0.371	0.367	1.011
20 cm	10 x 10	0.880	0.385	0.382	1.007
20 cm	15 x 15	0.962	0.410	0.407	1.008
20 cm	20 x 20	1.017	0.426	0.425	1.003
20 cm	30 x 30	1.083	0.445	0.448	0.993
20 cm	40 x 40	1.109	0.453	0.457	0.990

Table 10. Summary of the PDD values for the Clinac 4.

Depth (cm)	FS_{coll} (cm)	Average readings x TPC	PDD	PDD Used at MBPCC	Ratio= Measured/Used
1.2 cm	5 x 5	2.162	1.000	1.000	1.000
1.2 cm	6 x 6	2.189	1.000	1.000	1.000
1.2 cm	8 x 8	2.229	1.000	1.000	1.000
1.2 cm	10 x 10	2.263	1.000	1.000	1.000
1.2 cm	15 x 15	2.329	1.000	1.000	1.000
1.2 cm	20 x 20	2.373	1.000	1.000	1.000
1.2 cm	30 x 30	2.411	1.000	1.000	1.000
5 cm	5 x 5	1.724	0.797	0.797	1.000
5 cm	6 x 6	1.764	0.806	0.804	1.002
5 cm	8 x 8	1.806	0.810	0.817	0.992
5 cm	10 x 10	1.854	0.819	0.826	0.992
5 cm	15 x 15	1.942	0.834	0.837	0.996
5 cm	20 x 20	1.999	0.842	0.844	0.998
5 cm	30 x 30	2.056	0.853	0.852	1.001
10 cm	5 x 5	1.202	0.556	0.559	0.994
10 cm	6 x 6	1.245	0.569	0.571	0.996
10 cm	8 x 8	1.305	0.586	0.591	0.991
10 cm	10 x 10	1.364	0.603	0.607	0.993
10 cm	15 x 15	1.468	0.630	0.631	0.999
10 cm	20 x 20	1.532	0.646	0.651	0.992
10 cm	30 x 30	1.609	0.668	0.665	1.004

Continuing Table 10. Summary of the PDD values for the Clinac 4.

Depth (cm)	FS_{coll} (cm)	Average readings x TPC	PDD	PDD Used at MBPCC	Ratio= Measured/Used
1.2 cm	5 x 5	2.162	1.000	1.000	1.000
1.2 cm	6 x 6	2.189	1.000	1.000	1.000
1.2 cm	8 x 8	2.229	1.000	1.000	1.000
1.2 cm	10 x 10	2.263	1.000	1.000	1.000
1.2 cm	15 x 15	2.329	1.000	1.000	1.000
1.2 cm	20 x 20	2.373	1.000	1.000	1.000
1.2 cm	30 x 30	2.411	1.000	1.000	1.000
15 cm	5 x 5	0.834	0.386	0.390	0.988
15 cm	6 x 6	0.870	0.397	0.402	0.989
15 cm	8 x 8	0.927	0.416	0.422	0.986
15 cm	10 x 10	0.979	0.433	0.439	0.985
15 cm	15 x 15	1.086	0.466	0.469	0.994
15 cm	20 x 20	1.155	0.487	0.488	0.997
15 cm	30 x 30	1.234	0.512	0.511	1.002
20 cm	5 x 5	0.579	0.268	0.272	0.984
20 cm	6 x 6	0.607	0.277	0.282	0.984
20 cm	8 x 8	0.655	0.294	0.298	0.985
20 cm	10 x 10	0.701	0.309	0.313	0.989
20 cm	15 x 15	0.795	0.341	0.344	0.992
20 cm	20 x 20	0.858	0.362	0.364	0.993
20 cm	30 x 30	0.931	0.386	0.386	1.000

The tissue maximum ratio (TMR) measurements for the Clinac 600C were found to be within plus or minus two percent of the standard MBPCC dosimetric values. The TMR measurements were not taken for the Clinac 4 because the PDD technique is the preferred technique for the Clinac 4. Tables 11 on the following pages show the results of the average measurements taken compared to the standard MBPCC dosimetric values.

Table 11. Summary of the TMR values for the Clinac 600C.

Depth (cm)	FS_{coll} (cm)	Average readings x TPC	TMR	TMR Used at MBPCC	Ratio= Measured/Used
1.5 cm	5 x 5	2.237	1.000	1.000	1.000
1.5 cm	8 x 8	2.297	1.000	1.000	1.000
1.5 cm	10 x 10	2.339	1.000	1.000	1.000
1.5 cm	15 x 15	2.421	1.000	1.000	1.000
1.5 cm	20 x 20	2.474	1.000	1.000	1.000
1.5 cm	30 x 30	2.540	1.000	1.000	1.000
1.5 cm	40 x 40	2.579	1.000	1.000	1.000
5 cm	5 x 5	2.048	0.916	0.915	1.001
5 cm	8 x 8	2.149	0.936	0.928	1.008
5 cm	10 x 10	2.171	0.928	0.937	0.991
5 cm	15 x 15	2.260	0.933	0.943	0.989
5 cm	20 x 20	2.318	0.937	0.946	0.990
5 cm	30 x 30	2.399	0.944	0.949	0.995
5 cm	40 x 40	2.443	0.947	0.952	0.995
10 cm	5 x 5	1.677	0.749	0.760	0.986
10 cm	8 x 8	1.761	0.767	0.778	0.985
10 cm	10 x 10	1.828	0.782	0.793	0.986
10 cm	15 x 15	1.943	0.803	0.815	0.985
10 cm	20 x 20	2.015	0.814	0.821	0.992
10 cm	30 x 30	2.117	0.833	0.843	0.989
10 cm	40 x 40	2.171	0.842	0.849	0.992

Continuing Table 11. Summary of the TMR values for the Clinac 600C.

Depth (cm)	FS_{coll} (cm)	Average readings x TPC	TMR	TMR Used at MBPCC	Ratio= Measured/Used
1.5 cm	5 x 5	2.251	1.000	1.000	1.000
1.5 cm	8 x 8	2.320	1.000	1.000	1.000
1.5 cm	10 x 10	2.352	1.000	1.000	1.000
1.5 cm	15 x 15	2.411	1.000	1.000	1.000
1.5 cm	20 x 20	2.454	1.000	1.000	1.000
1.5 cm	30 x 30	2.506	1.000	1.000	1.000
1.5 cm	40 x 40	2.521	1.000	1.000	1.000
15 cm	5 x 5	1.329	0.591	0.587	1.006
15 cm	8 x 8	1.449	0.625	0.621	1.006
15 cm	10 x 10	1.511	0.642	0.639	1.005
15 cm	15 x 15	1.627	0.675	0.672	1.004
15 cm	20 x 20	1.707	0.696	0.692	1.005
15 cm	30 x 30	1.808	0.721	0.718	1.005
15 cm	40 x 40	1.851	0.734	0.732	1.003
20 cm	5 x 5	1.059	0.470	0.465	1.012
20 cm	8 x 8	1.166	0.503	0.497	1.011
20 cm	10 x 10	1.225	0.521	0.516	1.009
20 cm	15 x 15	1.341	0.556	0.552	1.008
20 cm	20 x 20	1.426	0.581	0.578	1.005
20 cm	30 x 30	1.538	0.614	0.613	1.001
20 cm	40 x 40	1.589	0.631	0.630	1.001

The tray factor (TF) measurements for the Clinac 600C and Clinac 4 were found to be within plus or minus two percent of the MBPCC dosimetric values used. Tables 12 and 13 show the results of the measurements taken compared to the MBPCC dosimetric values used.

Table 12. Summary of the tray factor values for the Clinac 600C.

Point Number	FS_{coll} (cm) 10 x 10	Depth (cm)	Average Reading x TPC	Tray Factor	Tray Factor used at MBPCC	Ratio = Measured/Used
1	Open (no tray)	5.0	1.949	1.000	1.000	1.000
2	Custom block tray	5.0	1.886	0.968	0.969	0.999

Table 13. Summary of the tray factor values for the Clinac 4.

Point Number	FS_{coll} (cm) 10 x 10	Depths (cm)	Average Reading x TPC	Tray Factor	Tray Factor used at MBPCC	Ratio = Measured/Used
1	Open (no tray)	5.0	1.849	1.000	1.000	1.000
2	Custom block tray	5.0	1.775	0.959	0.961	0.998

The hand and Cap-Plan computer comparison was done to have a quality assurance check against the Cap-Plan computer generated data, and to become more familiar with estimating the effective field size in dosimetry treatment planning.

The following tables 14 through 17 show the results of the hand and Cap-Plan computer comparison. The actual hand calculations are found in the appendix A: Hand Calculations. The method used to judge the effective field size for hand calculations was Khan's "approximation method" (1973).

Khan's "approximation method" is not being suggested as an alternative quality assurance check for radiation treatment facilities but one that I found comfortable with to use. Out of fifty points checked, forty-eight were calculated to be within plus or minus two percent of the Cap-Plan computer generated data. Two points at the lower mediastinum on a modified mantle case were calculated within three percent of computer generated data. Khan (1973) had reported that the approximation method he developed was good within plus or minus three percent. Van Dyk, et al. (1993) stipulated that manual checks should agree within plus or minus three percent of computer calculations.

Table 14. Comparison of test case T13529 hand calculations and computed data. (*)

Point Number	Site**	Depth	FS_{eff}	Hand Calculation	Computer Calculation	Ratio of Hand and Computer Calculation
1	CAXML	10.5 cm	14.9 cm^2	62.0 cGy	62.1 cGy	0.998
2	CAXDM	1.2 cm	14.9 cm^2	100.2 cGy	100.6 cGy	0.996
3	CAX/5	5.0 cm	14.9 cm^2	83.8 cGy	84.5 cGy	0.992
4	MMEDML	10.5 cm	13.7 cm^2	66.1 cGy	67.2 cGy	0.984
5	MMED/5	5.0 cm	13.7 cm^2	89.9 cGy	91.6 cGy	0.981
6	LMEDML	11.75 cm	10.5 cm^2	60.9 cGy	61.3 cGy	0.993
7	LMED/5	5.0 cm	10.5 cm^2	91.6 cGy	92.3 cGy	0.992
8	LAXML	10.0 cm	12.3 cm^2	70.5 cGy	69.2 cGy	1.019
9	LNECKM	9.5 cm	14.2 cm^2	72.2 cGy	71.8 cGy	1.006
10	CORD	10.0 cm	13.3 cm^2	82.4 cGy	81.9 cGy	1.006

* Field Description: AP Mini Mantle; Treatment Unit: Varian-Clinac 4/80; Central-Axis SSD: 80.0 cm; X Collimator: 29.0 cm; Y Collimator: 20.0 cm; FScoll: 23.7 cm^2

** The site abbreviations are the most common used by MBPCC dosimetrist when naming treatment locations for irregular treatment plans. The abbreviations stand for Central Axis (CAX), Central Axis Dmax (CAXDM), Central Axis 5cm (CAX/5), Mid-Mediastinal Mid-Line (MMEDML), Lower Mediastinal Mid-Line (LMEDML), Lower Mediastinal 5 cm (LMED/5), Left Axilla Mid-Line (LAXML), Left Neck Mid-line (LNECKM), and Spinal Cord (Cord).

Table 15. Comparison of test case T12754 hand calculations and computed data. (*)

Point Number	Site**	Depth	FSeff	Hand Calculation	Computer Calculation	Ratio of Hand and Computer Calculation
1	CAXML	8.25 cm	19.8 cm^2	72.4 cGy	72.0 cGy	1.006
2	CAXDM	1.2 cm	19.8 cm^2	101.5 cGy	101.3 cGy	1.002
3	CAX/5	5.0 cm	19.8 cm^2	85.6 cGy	85.6 cGy	1.000
4	MMEDML	9.5 cm	12.0 cm^2	71.4 cGy	70.3 cGy	1.016
5	MMED/5	5.0 cm	8.3 cm^2	92.9 cGy	92.1 cGy	1.009
6	MMEDCD	13.5 cm	12.0 cm^2	55.5 cGy	54.8 cGy	1.013
7	AX	3.0 cm	9.5 cm^2	89.4 cGy	91.1 cGy	0.981
8	UMED	3.0 cm	14.1 cm^2	98.3 cGy	99.3 cGy	0.989
9	SC	3.5 cm	18.5 cm^2	102.7 cGy	102.7 cGy	1.000
10	MAXCD	6.5 cm	12.0 cm^2	85.6 cGy	85.4 cGy	1.002
11	NECK	9.0 cm	18.5 cm^2	75.0 cGy	75.6 cGy	0.992

* Field Description: AP "Modified Mantle"; Treatment Unit: Varian-Clinac 4/80; Central-Axis SSD: 80.0 cm; X Collimator: 28.0 cm; Y Collimator: 28.0 cm; FScoll: 28.0 cm^2

** The site abbreviations stand for Central Axis Mid-Line (CAXML), Central Axis Dmax (CAXDM), Central Axis 5cm (CAX/5), Mid-Mediastinal Mid-Line (MMEDML), Mid-Mediastinal 5 cm (MMED/5), Mid-Mediastinal Cord Dose (MMEDCD), Axilla (AX), Upper Mediastinal (UMED), Supraclavicular (SC), Maximum Cord Dose (MAXCD), and NECK (NECK).

Table 16. Comparison of test case T13700 hand calculations and computed data.(*)

Point Number	Site**	Depth	FSeff	Hand Calculation	Computer Calculation	Ratio of Hand and Computer Calculation
1	CAXML	9.0 cm	20.1 cm^2	74.3 cGy	74.4 cGy	0.999
2	CAXDM	1.5 cm	20.1 cm^2	101.6 cGy	102.3 cGy	0.993
3	CAX	13.0 cm	20.1 cm^2	61.4 cGy	61.1 cGy	1.005
4	UMEDML	7.25 cm	18.3 cm^2	83.6 cGy	83.1 cGy	1.006
5	UMEDDM	1.5 cm	18.3 cm^2	105.3 cGy	105.4 cGy	0.999
6	UMED	9.5 cm	18.3 cm^2	74.9 cGy	74.8 cGy	1.001
7	MMEDML	9.5 cm	14.8 cm^2	73.8 cGy	73.9 cGy	0.999
8	MMED	14.0 cm	14.8 cm^2	58.5 cGy	58.7 cGy	0.997
9	LMEDML	9.5 cm	13.4 cm^2	73.7 cGy	72.2 cGy	1.021
10	LMED	14.0 cm	13.4 cm^2	58.1 cGy	56.4 cGy	1.030
11	MASSML	8.5 cm	16.9 cm^2	77.4 cGy	78.1 cGy	0.991
12	MASS	12.0 cm	16.9 cm^2	65.3 cGy	65.8 cGy	0.992
13	SC	7.5 cm	13.3 cm^2	81.5 cGy	82.0 cGy	0.994

* Field Description: AP Mini Mantle; Treatment Unit: 6 MV Photon Beam/600C; Central-Axis SSD: 91.0 cm; X Collimator: 23.97 cm; Y Collimator: 29.67 cm; FScoll: 26.5 cm^2

** The site abbreviations not mentioned before stand for Upper-Mediastinal Mid-Line (UMEDML), Upper-Mediastinal Dmax (MMEDDM), Upper-Mediastinal (UMED), Lower Mediastinal (LMED), Tumor Mass Mid-Line (MASSML), and Tumor Mass (MASS)

Table 17. Comparison of test case T13506 hand calculations and computed data. (*)

Point Number	Site**	Depth	FSeff	Hand Calculation	Computer Calculation	Ratio of Hand and Computer Calculation
1	CAXML	8.0 cm	25.1 cm^2	79.2 cGy	80.0 cGy	0.990
2	CAX/4	4.0 cm	25.1 cm^2	93.9 cGy	94.2 cGy	0.997
3	CAXCD	10.0 cm	25.1 cm^2	72.2 cGy	73.4 cGy	0.984
4	MMEDML	9.5 cm	16.0 cm^2	74.6 cGy	75.7 cGy	0.985
5	MMED/4	4.0 cm	16.0 cm^2	96.2 cGy	96.5 cGy	0.997
6	MMEDCD	14.0 cm	16.0 cm^2	59.5 cGy	60.6 cGy	0.982
7	LMEDML	10.6 cm	10.6 cm^2	68.4 cGy	67.4 cGy	1.015
8	LMED/4	4.0 cm	10.6 cm^2	94.8 cGy	94.7 cGy	1.001
9	LMEDCD	15.5 cm	10.6 cm^2	51.7 cGy	51.5 cGy	1.004
10	UMEDML	6.6 cm	16.5 cm^2	86.1 cGy	87.1 cGy	0.989
11	UMED/4	4.0 cm	16.5 cm^2	96.2 cGy	96.9 cGy	0.993
12	UMEDCD	6.5 cm	16.5 cm^2	87.2 cGy	88.4 cGy	0.986
13	RUPNEC	5.0 cm	16.5 cm^2	93.1 cGy	93.4 cGy	0.997
14	LMDNCK	5.25 cm	16.5 cm^2	91.1 cGy	92.3 cGy	0.987
15	LSC/3	3.0 cm	16.5 cm^2	100.1 cGy	100.2 cGy	0.999
16	RAXML	7.25 cm	11.5 cm^2	83.1 cGy	83.1 cGy	1.000

* Field Description: AP Mantle; Treatment Unit: 6 MV Photon Beam/600C; Central-Axis SSD: 100.0 cm; X Collimator: 37.0 cm; Y Collimator: 29.5 cm; FScoll: 32.8 cm^2

** The site abbreviations not mentioned before stand for Left Middle Neck (LMDNCK), Left Supra-clavicular 3 cm (LSC/3), and Right Axilla Mid-Line (RAXML)

The measured data and Capintec computer comparison was done to check the Capintec computer generated data against measured dose output in phantom using mantle field blocking. The results of this testing are shown in tables 18 through 21..

Table 18. Comparison of test case T13529 measurements and computed data. (*)

Point Number	Site	Depth	FS_{eff}	Measured Data	Computer Calculation	Ratio of Measured data and Computer Calculation
1	CAXML	10.5 cm	14.9 cm^2	62.8 cGy	62.1 cGy	1.011
2	CAXDM	1.2 cm	14.9 cm^2	102.6 cGy	100.6 cGy	1.019
3	CAX/5	5.0 cm	14.9 cm^2	85.2 cGy	84.5 cGy	1.009
4	MMEDML	10.5 cm	13.7 cm^2	65.9 cGy	67.2 cGy	0.982
5	MMED/5	5.0 cm	13.7 cm^2	90.2 cGy	91.6 cGy	0.984
6	LMEDML	11.75 cm	10.5 cm^2	60.8 cGy	61.3 cGy	0.993
7	LMED/5	5.0 cm	10.5 cm^2	91.3 cGy	92.3 cGy	0.989
8	LAXML	10.0 cm	12.3 cm^2	70.5 cGy	69.2 cGy	1.019
9	LNECKM	9.5 cm	14.2 cm^2	71.2 cGy	71.8 cGy	0.991
10	CORD	10.0 cm	13.3 cm^2	80.7 cGy	81.9 cGy	0.986

* Field Description: AP Mini Mantle; Treatment Unit: Varian-Clinac 4/80; Central-Axis SSD: 80.0 cm; X Collimator: 29.0 cm; Y Collimator: 20.0 cm; FScoll: 23.7 cm^2

Table 19. Comparison of test case T12754 measurements and computed data. (*)

Point Number	Site	Depth	FSeff	Measured Data	Computer Calculation	Ratio of Measured data and Computer Calculation
1	CAXML	8.25 cm	19.8 cm^2	72.8 cGy	72.0 cGy	1.011
2	CAXDM	1.2 cm	19.8 cm^2	103.2 cGy	101.3 cGy	1.019
3	CAX/5	5.0 cm	19.8 cm^2	86.6 cGy	85.6 cGy	1.012
4	MMEDML	9.5 cm	12.0 cm^2	70.9 cGy	70.3 cGy	1.008
5	MMED/5	5.0 cm	12.0 cm^2	93.1 cGy	92.1 cGy	1.011
6	MMEDCD	13.5 cm	12.0 cm^2	55.0 cGy	54.8 cGy	1.004
7	AX	3.0 cm	9.5 cm^2	89.5 cGy	91.1 cGy	0.982
8	UMED	3.0 cm	14.1 m^2	100.9 cGy	99.3 cGy	1.016
9	SC	3.5 cm	18.5 cm^2	103.1 cGy	102.7 cGy	1.004
10	MAXCD	6.5 cm	12.0 cm^2	85.4 cGy	85.4 cGy	1.000
11	NECK	9.0 cm	18.5 cm^2	75.2 cGy	75.6 cGy	0.995

* Field Description: AP "Modified Mantle"; Treatment Unit: Varian-Clinac 4/80; Central-Axis SSD: 80.0 cm; X Collimator: 28.0 cm; Y Collimator: 28.0 cm; FScoll: 28.0 cm^2

Table 20. Comparison of test case 13700 measurements and computed data. (*)

Point Number	Site	Depth	FSeff	Measured Data	Computer Calculation	Ratio of Measured Data and Computer Calculation
1	CAXML	9.0 cm	20.1 cm^2	74.6 cGy	74.4 cGy	1.002
2	CAXDM	1.5 cm	20.1 cm^2	103.1 cGy	102.3 cGy	1.008
3	CAX	13.0 cm	20.1 cm^2	60.9 cGy	61.1 cGy	0.998
4	UMEDML	7.25 cm	18.3 cm^2	82.4 cGy	83.1 cGy	0.992
5	UMEDDM	1.5 cm	18.3 cm^2	105.5 cGy	105.4 cGy	1.001
6	UMED	9.5 cm	18.3 cm^2	73.2 cGy	74.8 cGy	0.987
7	MMEDML	9.5 cm	14.8 cm^2	73.2 cGy	73.9 cGy	0.989
8	MMED	14.0 cm	14.8 cm^2	58.0 cGy	58.7 cGy	0.988
9	LMEDML	9.5 cm	13.4 cm^2	71.9 cGy	72.2 cGy	0.997
10	LMED	14.0 cm	13.4 cm^2	56.4 cGy	56.4 cGy	1.000
11	MASSML	8.5 cm	16.9 cm^2	77.9 cGy	78.1 cGy	0.997
12	MASS	12.0 cm	16.9 cm^2	65.9 cGy	65.8 cGy	1.001
13	SC	7.5 cm	13.3 cm^2	80.6 cGy	82.0 cGy	0.983

* Field Description: AP Mini Mantle; Treatment Unit: 6 MV Photon Beam/600C; Central-Axis SSD: 91.0 cm; X Collimator: 23.97 cm; Y Collimator: 29.67 cm; FScoll: 26.5 cm^2

Table 21. Comparison of test case 13506 measurements and computed data. (*)

Point Number	Site	Depth	FSeff	Measured Data	Computer Calculation	Ratio of Measured Data and Computer Calculation
1	CAXML	8.0 cm	25.1 cm^2	80.5 cGy	80.0 cGy	1.006
2	CAX/4	4.0 cm	25.1 cm^2	95.7 cGy	94.2 cGy	1.015
3	CAXCD	10.0 cm	25.1 cm^2	73.4 cGy	73.4 cGy	1.000
4	MMEDML	9.5 cm	16.0 cm^2	74.9 cGy	75.7 cGy	0.989
5	MMED/4	4.0 cm	16.0 cm^2	96.7 cGy	96.5 cGy	1.002
6	MMEDCD	14.0 cm	16.0 cm^2	59.9 cGy	60.6 cGy	0.989
7	LMEDML	10.6 cm	10.6 cm^2	67.6 cGy	67.4 cGy	1.004
8	LMED/4	4.0 cm	10.6 cm^2	94.8 cGy	94.7 cGy	1.002
9	LMEDCD	15.5 cm	10.6 cm^2	51.9 cGy	51.5 cGy	1.009
10	UMEDML	6.6 cm	16.5 cm^2	86.9 cGy	87.1 cGy	0.997
11	UMED/4	4.0 cm	16.5 cm^2	97.2 cGy	96.9 cGy	1.003
12	UMEDCD	6.5 cm	16.5 cm^2	88.3 cGy	88.4 cGy	0.999
13	RUPNEC	5.0 cm	16.5 cm^2	93.2 cGy	93.4 cGy	0.998
14	LMDNCK	5.25 cm	16.5 cm^2	92.8 cGy	92.3 cGy	1.006
15	LSC/3	3.0 cm	16.5 cm^2	101.0 cGy	100.2 cGy	1.008
16	RAXML	7.25 cm	11.5 cm^2	81.8 cGy	83.1 cGy	0.984

* Field Description: AP Mantle; Treatment Unit: 6 MV Photon Beam/600C; Central-Axis SSD: 100.0 cm; X Collimator: 37.0 cm; Y Collimator: 29.5 cm; FScoll: 32.8 cm^2

The mantle chair was not found to attenuate or change the 6 MV photon beam profile on the Clinac 600C as compared to the tennis racket support screen on the patient support apparatus. The measurements taken for FSDA, FSDP, NPSF, PDD, and TMR were measured at within plus or minus two percent of MBPCC dosimetric values.

Patients who actually used the mantle chair for Hodgkin's disease radiotherapy treatment planning found the positional comfortable. The first patient treated had a tumor size reduction shift of two and one half centimeters on the left lung sitting upright as compared to lying supine. Figure seven and eight on the following pages shows the before lying supine and the after sitting upright results. The upright positional device enhances the radiotherapy treatment plan when treating with the mantle field for Hodgkin's disease.

A side benefit not foreseen in using the upright positional device was observed in the treatment of lung cancer patients. Patients with non-Hodgkin's lymphomas or lung cancer patients sometimes experience mild to extreme discomfort when in a vertical position. By sitting upright, they are comfortable and are able to sit still longer for radiotherapy treatments and simulation procedures.

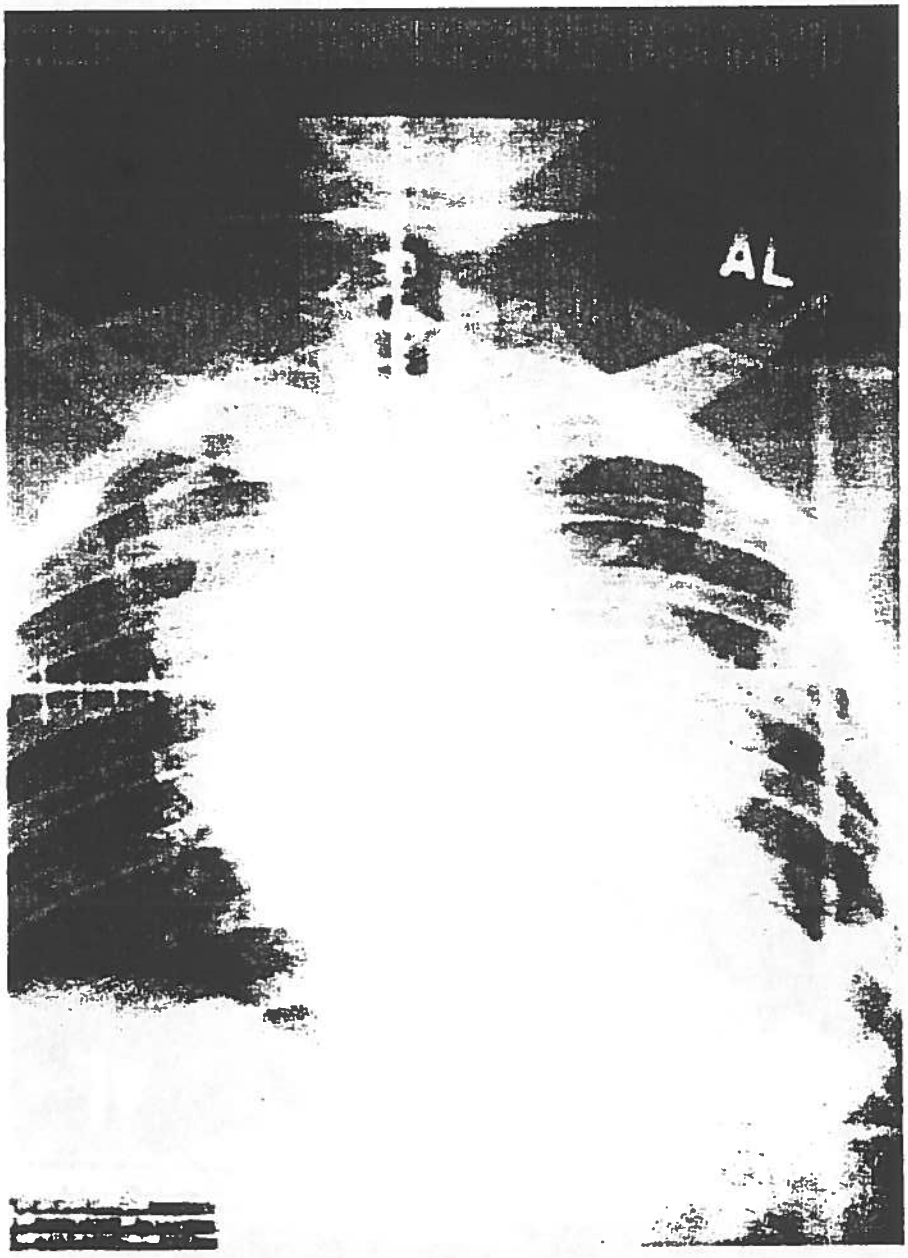

Figure 8. Anterior-posterior chest radiograph of a patient with mediastinal adenopathy showing the position of the mass from the a supine position.

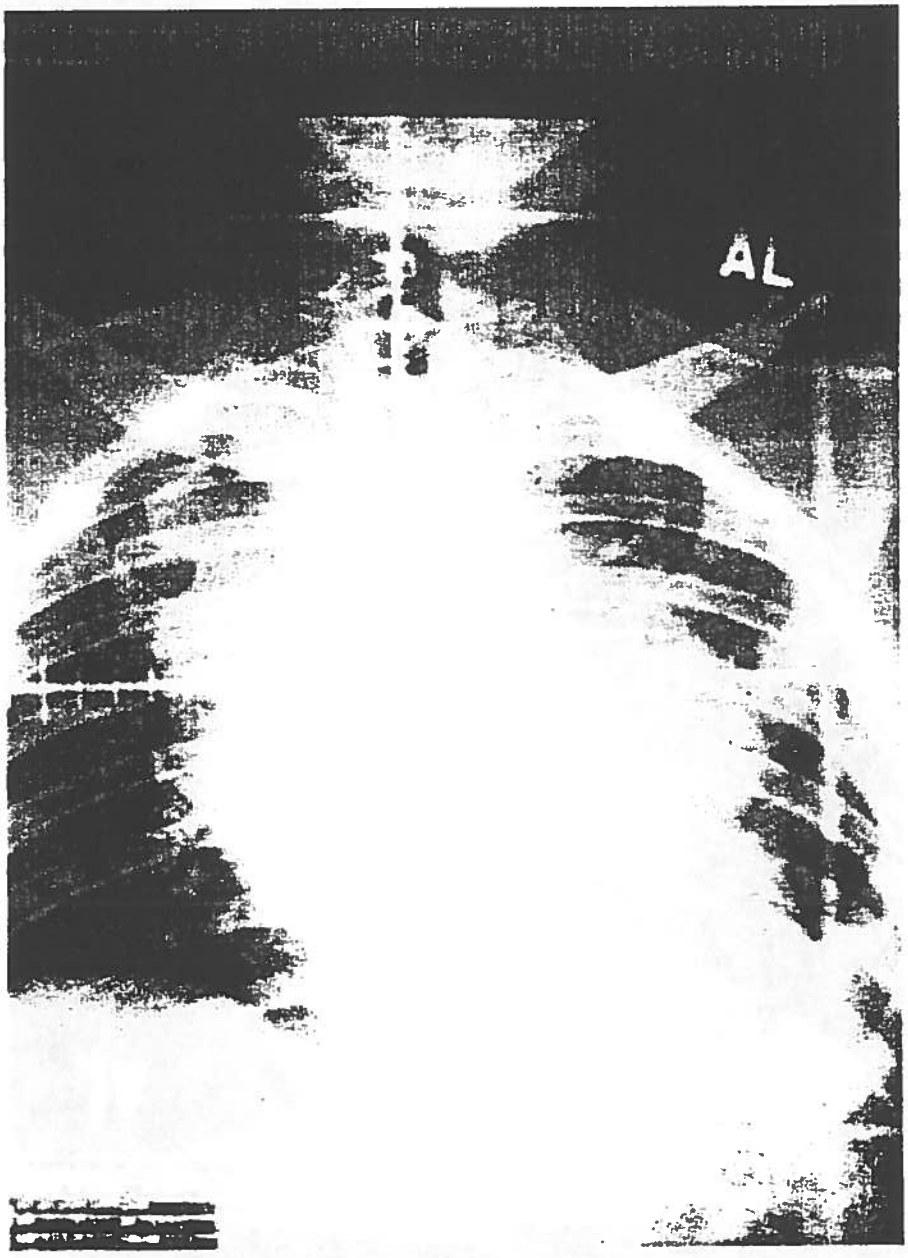

Figure 8. Anterior-posterior chest radiograph of a patient with mediastinal adenopathy showing the position of the mass from the a supine position.

Figure 9. Anterior-posterior chest radiograph of a patient with mediastinal adenopathy showing the shift of the tumor mass from the supine to the upright position.

Table 22. Summary of the FSDP values using the mantle chair for the Clinac 600C in phantom.

FS_{coll}	FSDP	FSDP Used at MBPCC	Ratio= Measured/Used
6 x 6	0.969	0.968	1.001
8 x 8	0.987	0.986	1.001
10 x 10	1.000	1.000	1.000
15 x 15	1.024	1.024	1.000
20 x 20	1.042	1.04	1.002
30 x 30	1.063	1.059	1.004
40 x 40	1.069	1.071	0.998

The SSD is 100 cm to the center of the chamber.

Table 23. Summary of the NPSF values using the mantle chair for the Clinac 600C.

FS_{coll}	FSDP	FSDA	NPSF*	NPSF Used at MBPCC	Ratio= Measured/Used
6 x 6	0.969	0.981	0.988	0.988	1.000
8 x 8	0.987	0.992	0.995	0.994	1.001
10 x 10	1.000	1.000	1.000	1.000	1.000
15 x 15	1.024	1.013	1.011	1.012	0.999
20 x 20	1.042	1.019	1.023	1.020	1.003
30 x 30	1.063	1.029	1.033	1.030	1.003
40 x 40	1.069	1.029	1.039	1.037	1.002

* Note: NPSF= FSDP/FSDA

Table 24. Summary of the PDD values using the mantle chair for the Clinac 600C.

Depth (cm)	FS_{coll} (cm)	Average readings x TPC	PDD	PDD Used at MBPCC	Ratio= Measured/Used
1.5 cm	5 x 5	2.191	1.000	1.000	1.000
1.5 cm	8 x 8	2.254	1.000	1.000	1.000
1.5 cm	10 x 10	2.285	1.000	1.000	1.000
1.5 cm	15 x 15	2.341	1.000	1.000	1.000
1.5 cm	20 x 20	2.380	1.000	1.000	1.000
1.5 cm	30 x 30	2.430	1.000	1.000	1.000
1.5 cm	40 x 40	2.447	1.000	1.000	1.000
5 cm	5 x 5	1.836	0.838	0.843	0.994
5 cm	8 x 8	1.923	0.853	0.853	1.000
5 cm	10 x 10	1.960	0.858	0.865	0.992
5 cm	15 x 15	2.025	0.865	0.872	0.992
5 cm	20 x 20	2.070	0.869	0.876	0.993
5 cm	30 x 30	2.126	0.875	0.881	0.993
5 cm	40 x 40	2.146	0.877	0.884	0.992
10 cm	5 x 5	1.361	0.621	0.626	0.992
10 cm	8 x 8	1.459	0.647	0.654	0.989
10 cm	10 x 10	1.508	0.659	0.667	0.989
10 cm	15 x 15	1.590	0.679	0.688	0.987
10 cm	20 x 20	1.642	0.689	0.698	0.988
10 cm	30 x 30	1.709	0.703	0.711	0.989
10 cm	40 x 40	1.736	0.709	0.716	0.991

Table 24. Continuing the PDD table summary using the mantle chair for the Clinac 600C.

Depth (cm)	FS_{coll} (cm)	Average readings x TPC	PDD	PDD Used at MBPCC	Ratio= Measured/Used
1.5 cm	5 x 5	2.139	1.000	1.000	1.000
1.5 cm	8 x 8	2.229	1.000	1.000	1.000
1.5 cm	10 x 10	2.274	1.000	1.000	1.000
1.5 cm	15 x 15	2.349	1.000	1.000	1.000
1.5 cm	20 x 20	2.401	1.000	1.000	1.000
1.5 cm	30 x 30	2.466	1.000	1.000	1.000
1.5 cm	40 x 40	2.508	1.000	1.000	1.000
15 cm	5 x 5	1.028	0.480	0.488	0.984
15 cm	8 x 8	1.131	0.507	0.512	0.991
15 cm	10 x 10	1.182	0.519	0.522	0.996
15 cm	15 x 15	1.276	0.543	0.543	1.000
15 cm	20 x 20	1.339	0.557	0.563	0.989
15 cm	30 x 30	1.415	0.574	0.574	1.000
15 cm	40 x 40	1.456	0.580	0.580	1.000
20 cm	5 x 5	0.765	0.358	0.364	0.983
20 cm	8 x 8	0.853	0.382	0.385	0.993
20 cm	10 x 10	0.899	0.395	0.391	1.011
20 cm	15 x 15	0.985	0.419	0.416	1.008
20 cm	20 x 20	1.045	0.435	0.430	1.012
20 cm	30 x 30	1.117	0.453	0.449	1.008
20 cm	40 x 40	1.153	0.459	0.456	1.008

Table 25. Summary of the TMR values using the mantle chair for the Clinac 600C.

Depth (cm)	FS_{coll} (cm)	Average readings x TPC	TMR	TMR Used at MBPCC	Ratio= Measured/Used
1.5 cm	5 x 5	2.251	1.000	1.000	1.000
1.5 cm	8 x 8	2.319	1.000	1.000	1.000
1.5 cm	10 x 10	2.351	1.000	1.000	1.000
1.5 cm	15 x 15	2.406	1.000	1.000	1.000
1.5 cm	20 x 20	2.449	1.000	1.000	1.000
1.5 cm	30 x 30	2.499	1.000	1.000	1.000
1.5 m	40 x 40	2.515	1.000	1.000	1.000
5 cm	5 x 5	2.023	0.899	0.902	0.997
5 cm	8 x 8	2.120	0.914	0.918	0.996
5 cm	10 x 10	2.1611	0.919	0.926	0.992
5 cm	15 x 15	2.234	0.928	0.934	0.994
5 cm	20 x 20	2.284	0.934	0.937	0.997
5 cm	30 x 30	2.346	0.939	0.941	0.998
5 cm	40 x 40	2.371	0.943	0.942	1.001
10 cm	5 x 5	1.639	0.728	0.726	1.003
10 cm	8 x 8	1.756	0.757	0.759	0.997
10 cm	10 x 10	1.814	0.772	0.777	0.994
10 cm	15 x 15	1.917	0.797	0.805	0.990
10 cm	20 x 20	1.985	0.811	0.818	0.991
10 cm	30 x 30	2.072	0.829	0.832	0.996
10 cm	40 x 40	2.109	0.839	0.839	1.000

Table 25. Continuing the TMR table summary using the mantle chair for the Clinac 600C.

Depth (cm)	FS_{coll} (cm)	Average readings x TPC	TMR	TMR Used at MBPCC	Ratio= Measured/Used
1.5 cm	5 x 5	2.241	1.000	1.000	1.000
1.5 cm	8 x 8	2.297	1.000	1.000	1.000
1.5 cm	10 x 10	2.337	1.000	1.000	1.000
1.5 cm	15 x 15	2.422	1.000	1.000	1.000
1.5 cm	20 x 20	2.472	1.000	1.000	1.000
1.5 cm	30 x 30	2.543	1.000	1.000	1.000
1.5 am	40 x 40	2.584	1.000	1.000	1.000
15 cm	5 x 5	1.381	0.616	0.625	0.986
15 cm	8 x 8	1.467	0.639	0.645	0.990
15 cm	10 x 10	1.532	0.656	0.661	0.992
15 cm	15 x 15	1.659	0.684	0.690	0.992
15 cm	20 x 20	1.743	0.705	0.708	0.996
15 cm	30 x 30	1.857	0.730	0.732	0.998
15 cm	40 x 40	1.915	0.741	0.741	1.000

CONCLUSIONS and RECOMMENDATIONS

The main objective of this thesis was to do a review of the mantle field technique at MBPCC, as well build an upright positional device. The results of the measured dose using mantle field technique on the Clinac 600C compared to the Capintec computer irregular field calculations were within plus or minus two percent of each other. This would confirm that the patients were receiving an accurate radiation treatment plan within the American College of Radiology standards. The mantle chair designed in this thesis was better than the previous positional device used at MBPCC. The old positional device was a bulky 121.92 by 243.84 cm sheet of 1.905 cm (4 by 8 feet sheet of 3/4 inch) plywood using an attached small wooden seat with two wooden dowels to position the patient's arms. The following comparisons are appropriate.

The old positional device was so bulky that it required a rented lift to position the patient for simulation and radiotherapy treatment. The new positional device does not require a rented lift.

The new positional device is more precise and easier to set up for treatment. With the faster set up time, the radiation therapists spent only allocated thirty minutes to treat the patient compared to one hour using the old positional device. The new positional device allows isocentric rotation where as the old positional device did not because of the tennis racket support used in the design.

The new positional device allows patients to be treated laterally for head and neck cancer. Patients who suffer discomfort laying down with non-lymphoma's in this particular case 'lung cancer' were under less stress when able to sit upright.

Patients are more comfortable during simulation and radiotherapy treatment because of the ergonomic designs incorporating a padded seat, padded elbow rest to position and help hold the weight of the arms, and a thermoplastic head positional c-frame to position the head, instead of using a dental bite block used in other mantle chair designs. These have the effect of relieving the physical stress upon the patient during the simulation, which can last as long as two hours.

The thermoplastic c-frame saves the patient the discomfort and cost of having the dental bite block made. This reduced the amount of time for the dosimetrist and therapists, so they could do other needed work. Since a bite block is not used, a dentist is not needed for this particular set up in most cases.

It is recommended that the dosimetrist make sure to mark the x-ray film where the points are being entered into the Capintec computer for irregular field size point calculations.

The dosimetrist needs to check that the lower mediastinum calculation point is the correct off-axis distance after completing the radiotherapy treatment plan. This distance checked will insure that the plan was done right if doing a TAD or a PDD treatment plan.

This mantle chair is a prototype that is currently being used to treat patients. The positional device can be improved on immediately in three areas: (1) constructed from wood, the weight of the positional device is seventy-five pounds. Lighter materials such as aluminum tube steel and acrylic plastic can be used to decrease the overall weight of the positional device by an estimated ten pounds. This would give a

greater margin in treating patients who are more increased in size than the standard person. The Clinac 600C patient support apparatus (PSA) can only lift a maximum of three hundred pounds. When you add the positional device to the PSA this only leaves you 225 pounds to work with. The elbow supports will have to be slightly redesigned using tube steel and acrylic but this should not present a problem. (2) the aesthetics of the wood being stained a dark color made some people uneasy. But this could be overcome by using aluminum or steel tubes and acrylic plastic to give a more modern "high-technology" appearance. (3) build a x-ray film holder attachment for the AP x-ray film to reduce the magnification factor of the film.

REFERENCES

Abrahamsen, A. Foss, and Host, H.(1981), "Mantle Field Irradiation for Stages 1A and 11A Hodgkin's Disease." *Scand J. Haematol* 26: 306-310.

American Association of Physicists in Medicine (AAPM) (1983), "A Protocol for the Determination of Absorbed Dose From High-Energy Photon and Electron Beams." *Medical Physics* 10 (November/December 1983).

Anderson, R.E., M.D., et al. (1969), "Dosimetry of Irregularly Shaped Radiation Therapy Fields Part 1: Some Factors Influencing Inhomogeneity." *Radiology* 92 (April 1969): 1092-1096.

Anderson, R.E., et al. (1969), "Dosimetry of Irregularly Shaped Radiation Therapy Fields Part 11: Isodose Contours Obtained Utilizing a Simulated Human Thorax." *Radiology* 92 (April 1969): 1097-1100.

Bagne, Farideh, PhD., and Dobebower, Ralph R., M.D., PhD. (1987), "Modified Mesh Panel for Radiation Therapy Treatment Table." *Radiology* 163: 579-580.

Behar, Robert A., and Hoppe, Richard T., M.D. (1990), "Radiation Therapy in the Management of Bulky Mediastinal Hodgkin's Disease." *Cancer* 66:75-79.

Bentel, Gunilla, R.N., R.T.T. (1991), "Positioning and Immobilization of Patients Undergoing Radiation Therapy for Hodgkin's Disease." *Medical Dosimetry* 16:111-117.

Boag, J.W., and Hodt, H.J. (1971),"Adjustable Chair for Radiotherapy of Head and Neck Cancer." *British Journal of Radiology* 44:316-317.

Bridier, A., et al. (1986), "A Comparison of Build-up and Depth Dose Characteristics of
Different Photon Beams for the Treatment of Hodgkin's Disease." *Radiotherapy and Oncology* 6: 301-307.

Byhardt, R., et al. (1975), "Dose and Treatment Factors in Radiation Related Pericardial Effusion Associated with the Mantle Technique for Hodgkin's Disease." *Cancer* 35:795-802.

Carmel, Richard J., M.D., and Kaplan, Henry S., M.D. (1976), "Mantle Irradiation in Hodgkin's Disease, An Analysis of Technique, Tumor Eradication, and Complications." *Cancer* 37: 2813-282.

Cilliers, G.D., et al. (1987), "A Study of the Mantle Technique for Hodgkin's Disease Using Thermoluminescent Dosimetry." *Radiotherapy and Oncology* 10:321-326.

Clarkson, J.R., PhD (1941), "A Note on Depth Doses in Fields of Irregular Shape." *British Journal of Radiology* 14 (164) (August 1941):265-268.

Cundiff, J.H., et al. (1973), "A Method for the Calculation of Dose in the Radiation Treatment of Hodgkin's Disease." *American Journal of Roentgenology-Radium Therapy and Nuclear Medicine* 117 (1) (January 1973): 30-44.

Gerber, Russell L., et al. (1982), "The Use of Thermal Plastics for Immobilization of Patients During Radiotherapy." *Int. J. Radiation Oncology Biol. Phys.* 8 (August 1982):1461-1462.

Gupta, S.K., M.Sc. and Cunningham, J.R., B.Eng., M.Sc., PhD. (1966), "Measurement of Tissue-Air Ratios and Scatter Functions for Large Field Sizes, for Cobalt 60 Gamma Radiation." *British Journal of Radiology* 39: 7-11 (January 1966).

Hanson, W.F. and Berkley, L.W. (1980), "Off-Axis Beam Quality Change in Linear Accelerators X-Ray Beams." *Medical Physics* 7 (2) (March/April 1980): 145-146.

Haus, A.G., et al. (1972), "A Film Technique for Determining the Absorbed Dose at Exit from the Patient During Radiation Exposure." *Radiology* 104 (July 1972):197-200.

Holleb, Arthur I., M.D., et al. (1991),"American Cancer Society Textbook of Clinical Oncology." The American Cancer Society, Inc.:377.

Holt, J. Garrett, et al. (1970), "The Extension of the Concept of Tissue-Air Ratios (TAR) to High-Energy X-ray Beams." *Radiology* 96 (August 1970): 437-446.

Hufton, A.P., and Russell, J.G.B. (1986), "The Use of Carbon Fibre Material in Table Tops, Cassette Fronts and Grid Covers: Magnitude of Possible Dose Reduction." *British Journal of Radiology* 59 (February 1986):157-163.

Hoppe, Richard, T.M.D. (1985), "The Management of Stage 11 Hodgkin's Disease With a Large Mediastinal Mass:A Prospective Program Emphasizing Irradiation." *Int. J. Radiation Oncology Biol. Phys.* 11: 349-355.

Khan, Faiz M., PhD (1970), "Computer Dosimetry of Partially Blocked Fields In Cobalt Teletherapy." Radiology 97 (November 1970): 405-411.

Khan, Faiz M., PhD (1994), "The Physics of Radiation Therapy." *Williams & Wilkins* Second Edition.

Khan, Faiz M., PhD., et al. (1973), "Computer and Approximation Methods of Calculating Depth Dose in Irregularly Shaped Fields." *Radiology* 106 (February 1973):433-436.

Khan, Faiz M., PhD., et al. (1986), "Dosimetry of Asymmetric X-ray Collimators." *Medical Physics* 13 (6) (November/December 1986):936-941.

Karzmark, C.J., et al. (1980), "A Versatile Radiotherapy Treatment Chair." *British Journal of Radiology* 53:1190-1194.

Kepka, Alan G., et al. (1985), "The Effect of Off-Axis Quality Changes on Zero Area TAR for Megavoltage Beams." *Physics in Medicine and Biology* 30 (6):589-595.

Kutcher, Gerald J., et al. (1994), "Comprehensive QA for radiation oncology: Report of AAPM Radiation Therapy Committee Task Group 40." *Medical Physics* 21 (4) (April 1994): 581-618.

Leopold, Kenneth A., et al. (1989), "Stage 1A-11B Hodgkin's Disease: Staging and Treatment of Patients With Large Mediastinal Adenopathy." *Journal of Clinical Oncology* 7 (August 1989):1059-1065.

Loshek, David D. (1988), "Analysis of Tissue-Maximum Ratio/Scatter-Maximum Ratio Model Relative to the Prediction of Tissue-Maximum Ratio in Asymmetrically Collimated Fields." *Medical Physics* 15 (5) (September/October 1988):672-682.

Marcial-Vega, V.A., M.D. (1990), et al., "Prevention of Hypothyroidism Related to Mantle Irradiation for Hodgkin's Disease: Preparative Phantom Study." *Int. J. Radiation Oncology Biol. Phys.* 18:613-618.

Marcus, Karen Chayt, et al. (1992), "Mantle Irradiation in the Upright Position: A Technique to Reduce the Volume of Lung Irradiation in Patients with Bulky Mediastinal Hodgkin's Disease." *Int J. Radiation Oncology Biol. Phys.* 23:443-447.

Meurk, Mary Louise, et al. (1968), "Phantom Dosimetry Study of Shaped Cobalt-60 Fields in the Treatment of Hodgkin's Disease." *Radiology* 91:554-558.

Mauch, Peter, M.D., et al. (1978), "The Significance Mediastinal Involvement in Early Stage Hodgkin's Disease." *Cancer* 42:1039-1045.

Mauch, Peter, M.D., and Buck, Beverly A., RT (R) (T) (1991), "The Treatment of Hodgkin's Disease Part 11: Radiation Therapy Techniques." *Forum Medicum, Inc.*

Palta, Jatinder R., PhD., et al. (1988), "Dosimetric Characteristics of a 6 MV Photon Beam from a Linear Accelerator with Asymmetric Collimator Jaws." *Int. J. Radiation Oncology Biol. Phys.* 14 (Feb. 1988):383-387.

Page, Vera, B.Sc., et al. (1970), "Physical and Dosimetric Aspects of the Radiotherapy of Malignant Lymphomas 1: The Mantle Technique." *Radiology* 96 (Sept 1970):609-618.

Sebaq-Montefiore, D.J. (1992), et al., "Variation in Mantle Technique: Implications for Establishing Priorities for Quality Assurance in Clinical Trials." *Radiotherapy and Oncology* 23:144-149.

Tarbell, Nancy J., M.D., et al. (1990),"Thoracic Irradiation in Hodgkin's Disease: Disease Control and Long-Term Complications." *Int. J. Radiation Oncology Biol. Phys.* 18:275-281.

Van Dyk, J., et al. (1993),"Commissioning and Quality Assurance of Treatment Planning
Computers." *Int. J. Radiation Oncology Biol. Phys.* 26 (2):261-273.

Wassermman, Todd H., et al. (1991), "Cure of Early-Stage Hodgkin's Disease with Subtotal Nodal Irradiation." *Cancer* 68:1208-1215.

Watson, G.A., Shuttle, E. and Deeley,T.J (1971),"A Radiotherapy Treatment Chair." *British Journal of Radiology* 48:317-319

Willett, Christopher G., M.D., et al. (1987),"The Effect of the Respiratory Cycle on Mediastinal and Lung Dimensions in Hodgkin's Disease." *Cancer* 60:1232-1237.

Worsnop, B. Ralph, M.A. (1968),"Phantom Thermoluminescent Dosimeter Comparison for a Cooperative Radiotherapy Trial." *Radiology* 91 (Sept 1968):545-553.

APPENDIX A: Hand Calculations

The appendix shows the diagrams of the mantle field blocking designs and hand calculations for four test cases. The hand calculations derive the effective field size from the diagrams using Khan's (1973) "approximation method". The hand calculation results are compared to the Cap-Plan computer generated data in the results section of this thesis. Equation 13 is used for the hand calculations. The effective field size and field size collimator were obtained by the equation $[2(Y \times X)/(Y + X)]$ to get an equivalent square. Where Y is the vertical length and X is the horizontal length of the field size.

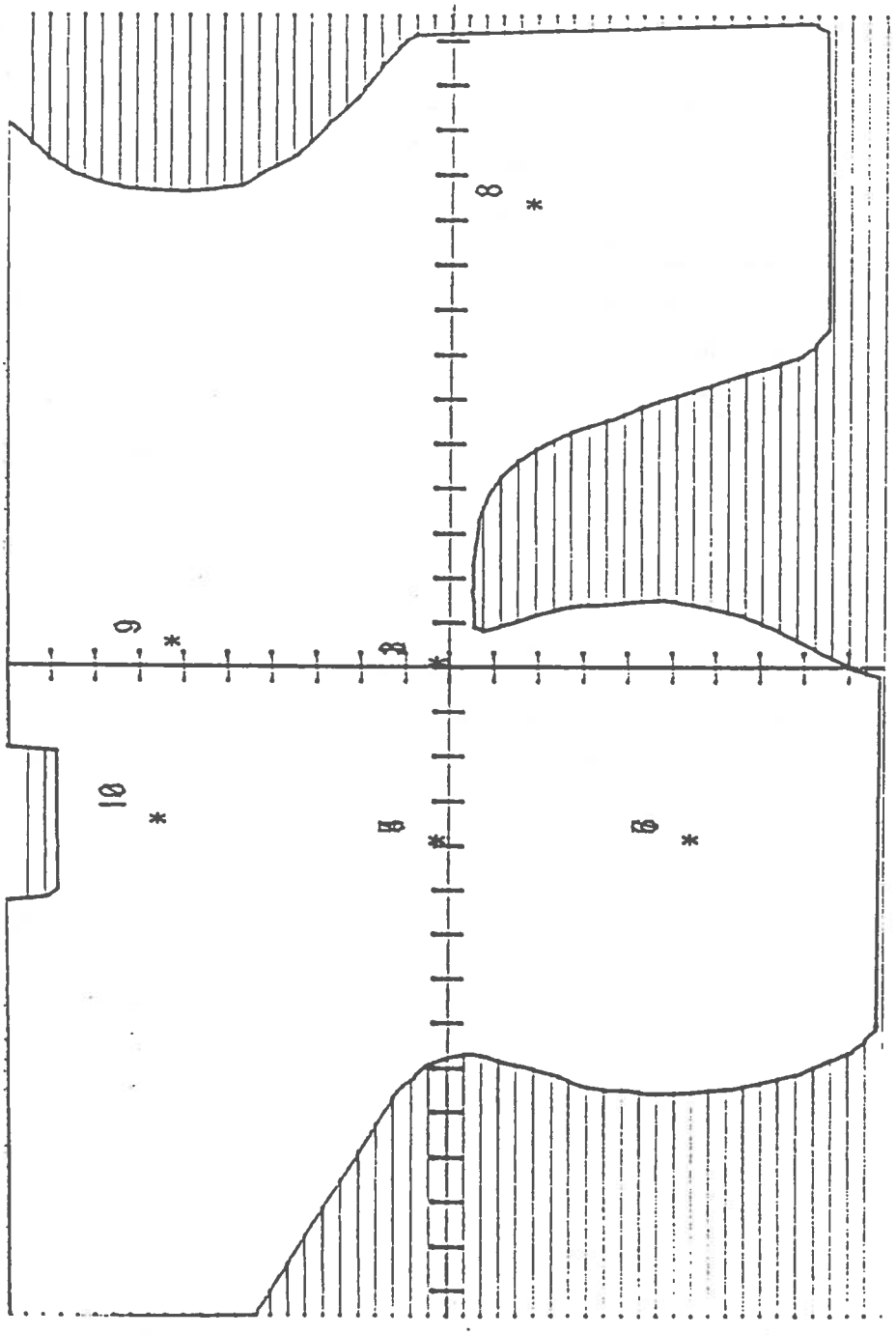

A.1. Diagram of mantle field test case T13529.

A.1. Hand calculation of output factors to CAX and to off-axis points for mantle field technique test case 13529. (*)

Point Number	1
Machine	Clinac-4
Site	CAXML
Description	Central-Axis
Field Size Collimator (cm^2)	2(19.7 X 29.1)/48.8= 23.5
Field Size Effective (cm^2)	2(10.4 X 26.7)/37.1= 14.9
Off Axis Distance	N/A
Depth (cm)	10.5
Field Size Dependence In Air (Collimator)	1.026
Off Axis Factor (Air)	N/A
Inverse Square	N/A
Normalized Peak Scatter Factor (Effective)	1.016
Depth Dose	0.618
Mayneord Factor	N/A
Tray Factor	0.961
Output Factor (rads/MU)	0.619
Monitor Units (100 MU) X Output Factor	62.0 cGy

* SSD: 80.0 cm; Field: AP

A.1. Hand calculation of output factors to CAX and to off-axis points for mantle field technique test case 13529. (*)

Point Number	1
Machine	Clinac-4
Site	CAXML
Description	Central-Axis
Field Size Collimator (cm^2)	2(19.7 X 29.1)/48.8= 23.5
Field Size Effective (cm^2)	2(10.4 X 26.7)/37.1= 14.9
Off Axis Distance	N/A
Depth (cm)	10.5
Field Size Dependence In Air (Collimator)	1.026
Off Axis Factor (Air)	N/A
Inverse Square	N/A
Normalized Peak Scatter Factor (Effective)	1.016
Depth Dose	0.618
Mayneord Factor	N/A
Tray Factor	0.961
Output Factor (rads/MU)	0.619
Monitor Units (100 MU) X Output Factor	62.0 cGy

* SSD: 80.0 cm; Field: AP

A.1. (Continued)

Point Number	2	3	4
Machine	Clinac-4	Clinac-4	Clinac-4
Site	CAXDM	CAX/5	MMEDML
Desciption	Central Axis	Central Axis	Med-Mediastinum
SSD (cm)	80.0	80.0	80.0
FScoll (cm^2)	23.5	23.5	23.5
FSeff (cm^2)	14.9	14.9	2(19.7 X 10.5)/30.2 = 13.7
OAD (cm)	N/A	N/A	4.0
Depth (cm)	1.2	5.0	10.5
FSDAcoll	1.026	1.026	1.026
OAFair	N/A	N/A	1.08
Inverse Square	N/A	N/A	N/A
NPSFeff	1.016	1.016	1.012
Depth Dose	1.0	0.837	0.613
Mayneord Factor	N/A	N/A	N/A
Tray Factor	0.961	0.961	0.961
Output Factor (rads/MU)	1.002	0.838	0.661
Monitor Units (100 MU) X Output Factor	100.2 cGy	83.8 cGy	66.1 cGy

A.1. (Continued)

Point Number	2	3	4
Machine	Clinac-4	Clinac-4	Clinac-4
Site	CAXDM	CAX/5	MMEDML
Desciption	Central Axis	Central Axis	Med-Mediastinum
SSD (cm)	80.0	80.0	80.0
FScoll (cm^2)	23.5	23.5	23.5
FSeff (cm^2)	14.9	14.9	2(19.7 X 10.5)/30.2 = 13.7
OAD (cm)	N/A	N/A	4.0
Depth (cm)	1.2	5.0	10.5
FSDAcoll	1.026	1.026	1.026
OAFair	N/A	N/A	1.08
Inverse Square	N/A	N/A	N/A
NPSFeff	1.016	1.016	1.012
Depth Dose	1.0	0.837	0.613
Mayneord Factor	N/A	N/A	N/A
Tray Factor	0.961	0.961	0.961
Output Factor (rads/MU)	1.002	0.838	0.661
Monitor Units (100 MU) X Output Factor	100.2 cGy	83.8 cGy	66.1 cGy

A.1. (Continued)

Point Number	5	6	7
Machine	Clinac-4	Clinac-4	Clinac-4
Site	MMED/5	LMEDML	LMED/5
Description	Mid-Mediastinum	Lower-Mediastinum	Lower-Mediastinum
SSD (cm)	80.0	80.0	80.0
FScoll (cm^2)	23.5	23.5	23.5
FSeff (cm^2)	13.7	2(10.0 X 11.0)/21 = 10.5	10.5
OAD (cm)	4.0	7.1	7.1
Depth (cm)	5.0	11.75	5.0
FSDAcoll	1.026	1.026	1.026
OAFair	1.08	1.12	1.12
Inverse Square	N/A	N/A	N/A
NPSFeff	1.012	1.002	1.002
Depth Dose	0.835	0.550	0.828
Mayneord Factor	N/A	N/A	N/A
Tray Factor	0.961	0.961	0.961
Output Factor (rads/MU)	0.899	0.609	0.916
Monitor Units (100 MU) X Output Factor	89.9 cGy	60.9 cGy	91.6 cGy

A.1. (Continued)

Point Number	8	9	10
Machine	Clinac-4	Clinac-4	Clinac-4
Site	LAXML	LNECK/5	Cord
Description	Axilla	Neck	Spinal Cord
SSD (cm)	80.0	80.0	80.0
FScoll (cm^2)	23.5	23.5	23.5
FSeff (cm^2)	2(19.7 X 9)/28.7 = 12.3	2(10.0 X 24.5)/34.5 = 14.2	2(19.7 X 10)/29.7 = 13.3
OAD (cm)	10.4	5.8	10.4
Depth (cm)	10.0	9.5	10.0
FSDAcoll	1.026	1.026	1.026
OAFair	1.14	1.11	1.12
Inverse Square	N/A	N/A	N/A
NPSFeff	1.007	1.013	1.01
Depth Dose	0.623	0.651	0.739
Mayneord Factor	N/A	N/A	N/A
Tray Factor	0.961	0.961	0.961
Output Factor (rads/MU)	0.705	0.722	0.824
Monitor Units (100MU) X Output Factor	70.5 cGy	72.2 cGy	82.4 cGy

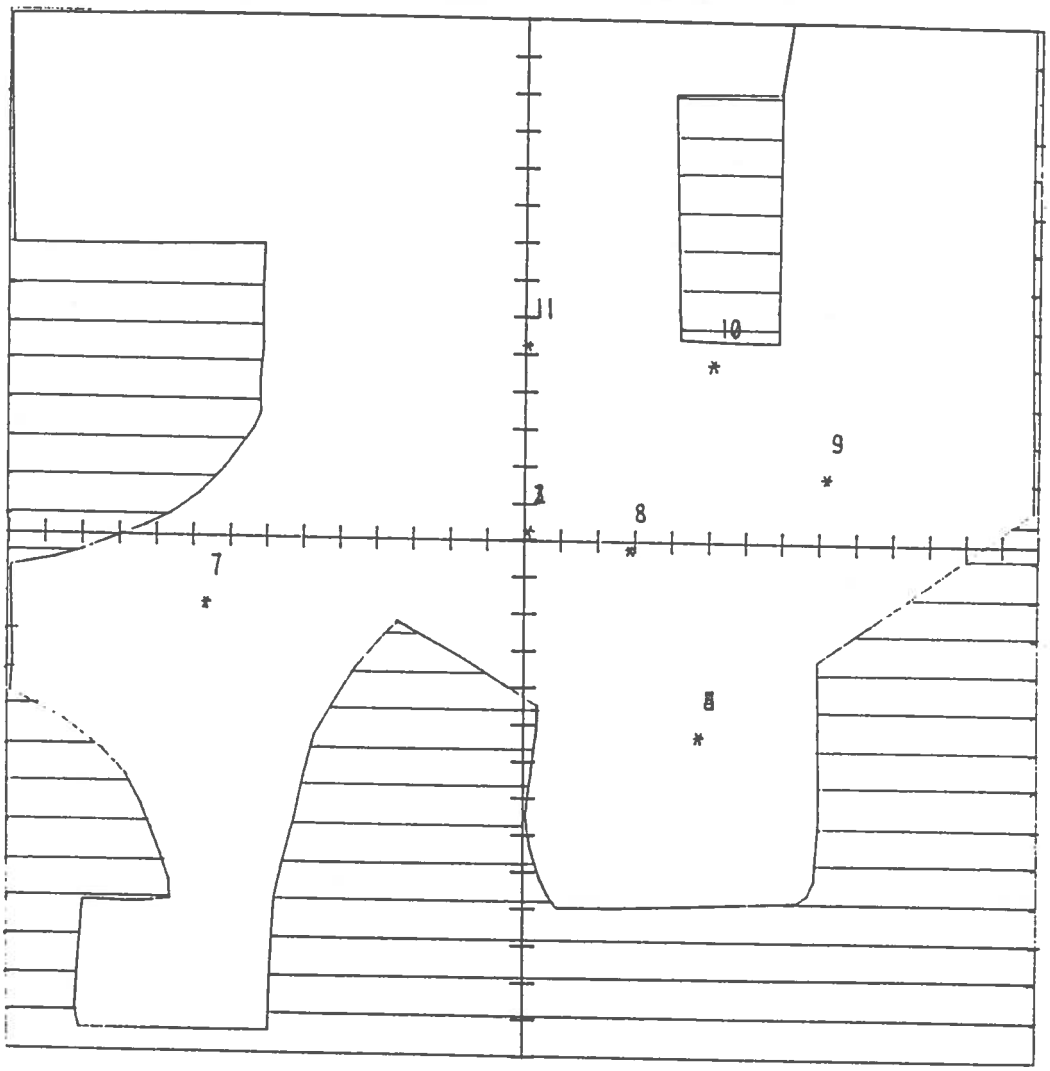

A.2. Diagram of mantle field test case T12754.

A.2. Hand calculation of output factors to CAX and to off-axis points for mantle field technique test case T12754. (*)

Point Number	1
Machine	Clinac-4
Site	CAXML
Description	Central-Axis
Field Size Collimator (cm^2)	2(28 X 28.2)/56.2= 28.1
Field Size Effective (cm^2)	2(18.0 X 22.0)/40.0 = 19.8
Off Axis Distance	N/A
Depth (cm)	8.25
Field Size Dependence In Air (Collimator)	1.03
Off Axis Factor (Air)	N/A
Inverse Square	N/A
Normalized Peak Scatter Factor (Effective)	1.025
Depth Dose	0.714
Mayneord Factor	N/A
Tray Factor	0.961
Output Factor (rads/MU)	0.724
Monitor Units (100 MU) X Output Factor	72.4 cGy

* SSD: 80.0 cm; Field: AP

A.2. (Continued)

Point Number	2	3	4
Machine	Clinac-4	Clinac-4	Clinac-4
Site	CAXDM	CAX/5	MMEDML
Description	Central-Axis	Central-Axis	Mid-Mediastinum
SSD (cm)	80.0	80.0	80.0
FScoll (cm^2)	28.0	28.0	28.0
FSeff (cm^2)	19.8	19.8	2(24.0 X 8.0)/32.0 = 12.0
OAD (cm)	N/A	7.1	7.1
Depth (cm)	1.2 cm	5.0	9.5
FSDAcoll	1.03	1.03	1.03
OAFair	N/A	N/A	1.12
Inverse Square	N/A	N/A	N/A
NPSFeff	1.025	1.025	1.007
Depth Dose	1.0	0.844	0.640
Mayneord Factor	N/A	N/A	N/A
Tray Factor	0.961	0.961	0.961
Output Factor (rads/MU)	1.015	0.856	0.714
Monitor Units (100 MU) * Output Factor	101.5 cGy	85.6 cGy	71.4 cGy

A.2. (Continued)

Point Number	5	6	7
Machine	Clinac-4	Clinac-4	Clinac-4
Site	MMED/5	MMEDCD	AX
Description	Mid-Mediastinum	Mid-Mediastinum	Axilla
SSD (cm)	80.0	80.0	80.0
FScoll (cm^2)	28.0	28.0	28.0
FSeff (cm^2)	12.0	12.0	2(9.0 X 10.0)/19.0 = 9.5
OAD (cm)	7.1	7.1	8.9
Depth (cm)	5.0	13.5	3.0
FSDAcoll	1.03	1.03	1.03
OAFair	1.12	1.12	1.13
Inverse Square	N/A	N/A	N/A
NPSFeff	1.007	1.007	0.998
Depth Dose	0.832	0.497	0.801
Mayneord Factor	N/A	N/A	N/A
Tray Factor	0.961	0.961	0.961
Output Factor (rads/MU)	0.929	0.555	0.894
Monitor Units (100 MU) X Output Factor	92.9 cGy	55.5 cGy	89.4 cGy

A.2. (Continued)

Point Number	8	9	10
Machine	Clinac-4	Clinac-4	Clinac-4
Site	UMED	SC	MAXCD
Description	Upper-Mediastinum	Supra-Clavicular	Spinal Cord
SSD (cm)	80.0	80.0	80.0
FScoll (cm^2)	28.0	28.0	28.0
FSeff (cm^2)	2(24.0 X 10)/34.0= 14.1	2(16.0 X 22.0)/ 8 = 18.5	2(24.0 X 8.0)/32.0 = 12.0
OAD (cm)	2.8	8.1	6.7
Depth (cm)	3.0	3.5	6.5
FSDAcoll	1.03	1.03	1.03
OAFair	1.06	1.12	1.12
Inverse Square	N/A	N/A	N/A
NPSFeff	1.013	1.018	1.007
Depth Dose	.925	0.910	0.767
Mayneord Factor	N/A	N/A	N/A
Tray Factor	0.961	0.961	0.961
Output Factor (rads/MU)	0.983	1.027	0.856
Monitor Units (100 MU) X Output Factor	98.3 cGy	102.7 cGy	85.6 cGy

A.2. (Continued)

Point Number	11
Machine	Clinac-4
Site	NECK
Description	NECK
SSD (cm)	80.0
FScoll (cm^2)	28.0
FSeff (cm^2)	2(16.0 X 22.0)/ 38.0 = 18.5
OAD (cm)	5.0
Depth (cm)	9.0
FSDAcoll	1.03
OAFair	1.09
Inverse Square	N/A
NPSFeff	1.018
Depth Dose	0.683
Mayneord Factor	N/A
Tray Factor	0.961
Output Factor (rads/MU)	0.750
Monitor Units (100 MU) * Output Factor	75.0 cGy

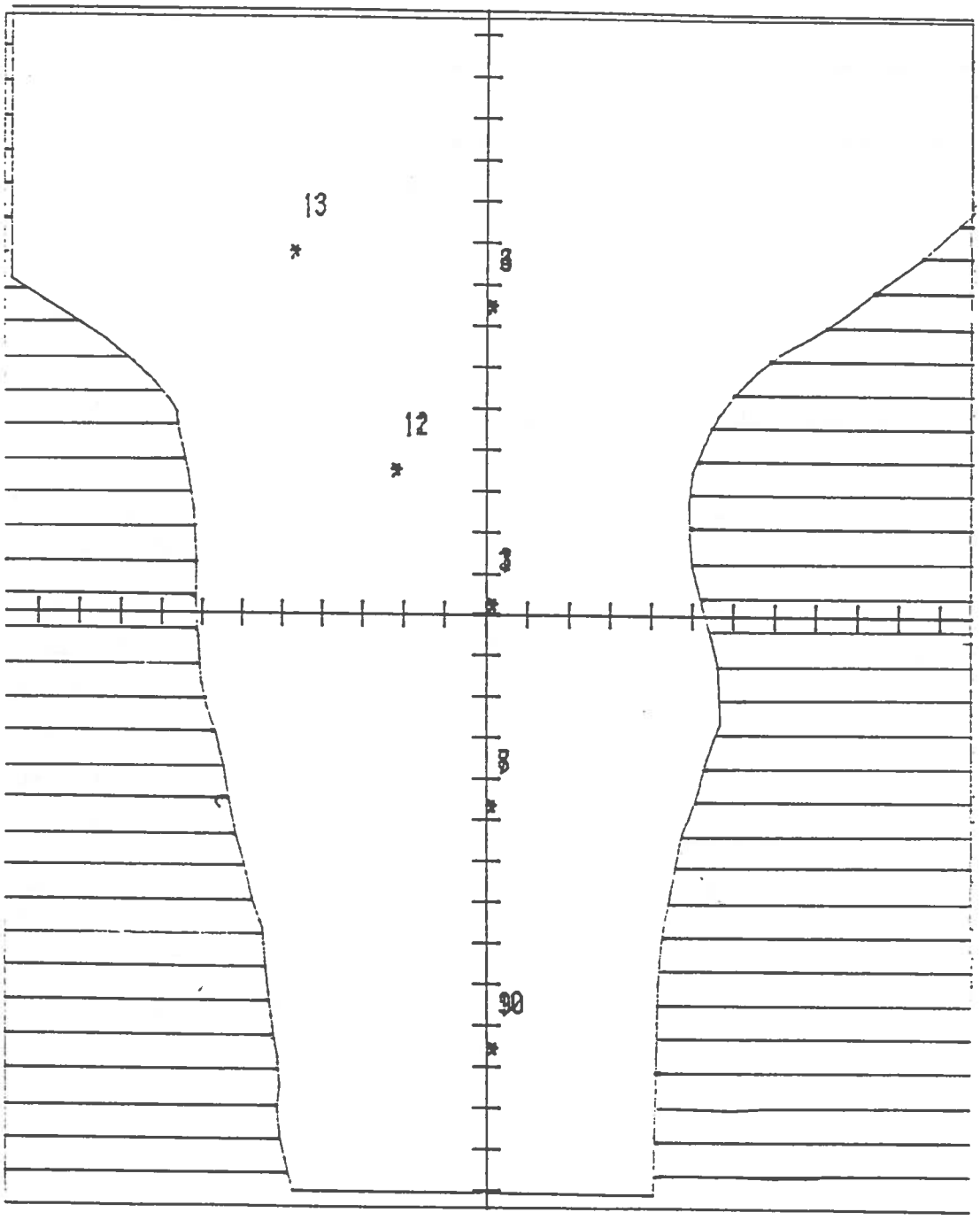

A.3. Diagram of mantle field test case 13700.

A.3. Hand calculation of output factors to CAX and to off-axis points for mantle field technique test case 13700. (*)

Point Number	1
Machine	Clinac-600C
Site	CAXML
Description	Central-Axis
Field Size Collimator (cm^2)	2(28.8 X 23.6)/52.4= 25.9
Field Size Effective (cm^2)	2(28.8 X 15.4)/44.2= 20.1
Off Axis Distance	N/A
Depth (cm)	9.0
Field Size Dependence In Air (Collimator)	1.027
Off Axis Factor (Air)	N/A
Inverse Square	N/A
Normalized Peak Scatter Factor (Effective)	1.021
Depth Dose	0.731
Mayneord Factor	N/A
Tray Factor	0.969
Output Factor (rads/MU)	0.743
Monitor Units (100 MU) X Output Factor	74.3 cGy

* SSD: 100.0 cm; Field: AP

A.3. (Continued)

Point Number	2	3	4
Machine	Clinac-600C	Clinac-600C	Clinac-600C
Site	CAXDM	CAX	UMEDML
Description	Central-Axis	Central-Axis	Upper-Mediastinum
SSD (cm)	100.0	100.0	100.0
FScoll (cm^2)	25.9	25.9	25.9
FSeff (cm^2)	20.1	20.1	2(28.8 X 12.7)/41.5= 18.3
OAD (cm)	N/A	N/A	7.2
Depth (cm)	1.5	13.0	7.25
FSDAcoll	1.027	1.027	1.027
OAFair	N/A	N/A	1.04
Inverse Square	N/A	N/A	N/A
NPSFeff	1.021	1.021	1.017
Depth Dose	1.0	0.604	0.794
Mayneord Factor	N/A	N/A	N/A
Tray Factor	0.969	0.969	0.969
Output Factor (rads/MU)	1.016	0.614	0.836
Monitor Units (100 MU) X Output Factor	101.6 cGy	61.4 cGy	83.6 cGy

A.3. (Continued)

Point Number	5	6	7
Machine	Clinac-600C	Clinac-600C	Clinac-600C
Site	UMEDDM	UMED	MMEDML
Description	Upper-Mediastinum	Upper-Mediastinum	Mid-Mediastinum
SSD (cm)	100.0	100.0	100.0
FScoll (cm^2)	26.5	26.5	26.5
FSeff (cm^2)	18.3	18.3	2(28.8 X 10.0)/ 38.8 = 14.8
OAD (cm)	7.2	7.2	4.9
Depth (cm)	1.5	9.5	9.5
FSDAcoll	1.027	1.027	1.027
OAFair	1.04	1.04	1.04
Inverse Square	N/A	N/A	N/A
NPSFeff	1.017	1.017	1.011
Depth Dose	1.0	0.712	0.705
Mayneord Factor	N/A	N/A	N/A
Tray Factor	0.969	0.969	0.969
Output Factor (rads/MU)	1.053	0.749	0.738
Monitor Units (100 MU) X Output Factor	105.3 cGy	74.9 cGy	73.8 cGy

A.3. (Continued)

Point Number	8	9	10
Machine	Clinac-600C	Clinac-600C	Clinac-600C
Site	MMED	LMEDML	LMEDP5
Description	Mid-Mediastinum	Lower-Mediastinum	Lower-Mediastinum
SSD (cm)	100.0	100.0	100.0
FScoll (cm^2)	26.5	26.5	26.5
FSeff (cm^2)	2(28.8 X 10.0)/38.8= 14.8	2(28.8 X 8.7)/ 37.5 = 13.4	13.4
OAD (cm)	4.9	10.8	10.8
Depth (cm)	14.0	9.5	14.0
FSDAcoll	1.027	1.027	1.027
OAFair	1.04	1.05	1.05
Inverse Square	N/A	N/A	N/A
NPSFeff	1.011	1.008	1.008
Depth Dose	0.559	0.700	0.552
Mayneord Factor	N/A	N/A	N/A
Tray Factor	0.969	0.969	0.969
Output Factor (rads/MU)	0.585	0.737	0.581
Monitor Units (100 MU) X Output Factor	58.5 cGy	73.7 cGy	58.1 cGy

A.3. (Continued)

Point Number	11	12	13
Machine	Clinac-600C	Clinac-600C	Clinac-600C
Site	MASSML	MASS	SC
Description	Tumor Mass	Tumor Mass	Supraclavicular
SSD (cm)	100.0	100.0	100.0
FScoll (cm^2)	26.5	26.5	26.5
FSeff (cm^2)	2(28.8 X 12.0)/40.8= 16.9	16.9	2(9.3 X 23.3)/ 32.6 = 13.3
OAD (cm)	4.4	4.4	10.8
Depth (cm)	8.5	12.0	7.5
FSDAcoll	1.027	1.027	1.027
OAFair	1.03	1.03	1.05
Inverse Square	N/A	N/A	N/A
NPSFeff	1.015	1.015	1.007
Depth Dose	0.744	0.628	0.775
Mayneord Factor	N/A	N/A	N/A
Tray Factor	0.969	0.969	0.969
Output Factor (rads/MU)	0.774	0.653	0.815
Monitor Units (100MU) X Output Factor	77.4 cGy	65.3 cGy	81.5 cGy

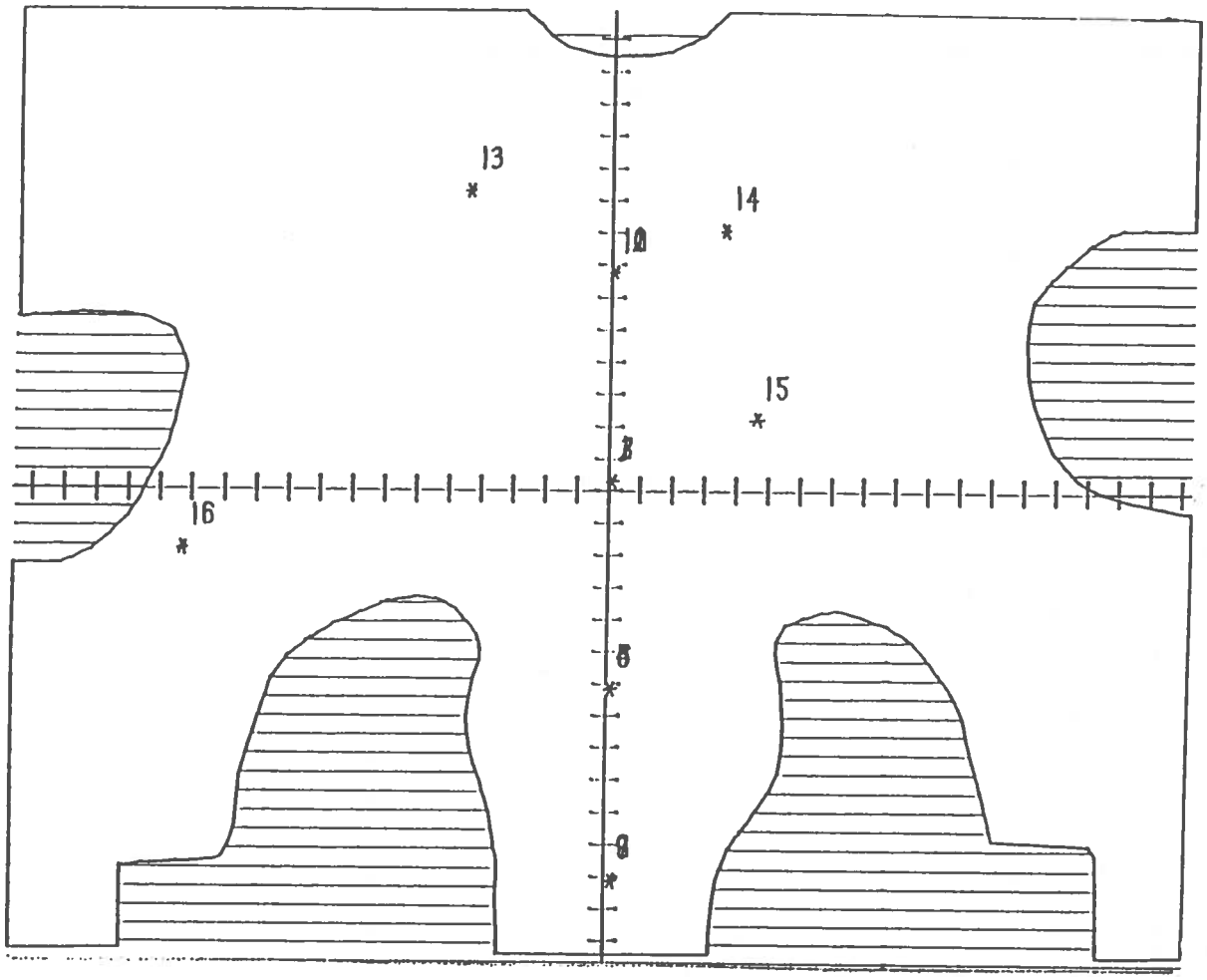

A.4. Diagram of mantle field test case 13506.

A.4. Hand calculation of output factors to CAX and to off-axis points for mantle field technique test case 13506. (*)

Point Number	1
Machine	Clinac-600C
Site	CAXML
Field Size Collimator (cm^2)	2(29.4 X 37)/66.4= 32.8
Field Size Effective (cm^2)	2(19 X 37)/56.0= 25.1
Off Axis Distance	N/A
Depth (cm)	8.0
Field Size Dependence In Air (Collimator)	1.032
Off Axis Factor (Air)	N/A
Inverse Square	N/A
Normalized Peak Scatter Factor (Effective)	1.026
Depth Dose	0.772
Mayneord Factor	N/A
Tray Factor	0.969
Output Factor (rads/MU)	0.792
Monitor Units (100 MU) X Output Factor	79.2 cGy

* SSD: 100.0 cm; Field: AP

A.4. (Continued)

Point Number	2	3	4
Machine	Clinac-600C	Clinac-600C	Clinac-600C
Site	CAX/4	CAXCD	MMEDML
Description	Central-Axis	Central-Axis	Mid-Mediastinum
SSD (cm)	100.0	100.0	100.0
FScoll (cm^2)	32.8	32.8	32.8
FSeff (cm^2)	25.1	25.1	2(29.5 X 11)/ 40.5 = 16.0
OAD (cm)	N/A	N/A	6.5
Depth (cm)	4.0	10.0	9.5
FSDAcoll	1.032	1.032	1.032
OAFair	N/A	N/A	1.04
Inverse Square	N/A	N/A	N/A
NPSFeff	1.026	1.026	1.014
Depth Dose	0.915	0.705	0.709
Mayneord Factor	N/A	N/A	N/A
Tray Factor	0.969	0.969	0.969
Output Factor (rads/MU)	0.939	0.722	0.746
Monitor Units (100 MU) X Output Factor	93.9 cGy	72.2 cGy	74.6 cGy

A.4. (Continued)

Point Number	5	6	7
Machine	Clinac-600C	Clinac-600C	Clinac-600C
Site	MMED/4	MMEDCD	LMEDML
Description	Mid-Mediastinum	Mid-Mediastinum	Lower-Mediastinum
SSD (cm)	100.0	100.0	100.5
FScoll (cm^2)	32.8	32.8	32.8
FSeff (cm^2)	16.0	16.0	2(29.4 X 6.5)/ 35.9 = 10.6
OAD (cm)	6.5	6.5	12.5
Depth (cm)	4.0	14.0	10.6
FSDAcoll	1.032	1.032	1.032
OAFair	1.04	1.04	1.05
Inverse Square	N/A	N/A	N/A
NPSFeff	1.014	1.014	1.002
Depth Dose	0.912	0.565	0.650
Mayneord Factor	N/A	N/A	N/A
Tray Factor	0.969	0.969	0.969
Output Factor (rads/MU)	0.962	0.595	0.684
Monitor Units (100 MU) X Output Factor	96.2 cGy	59.5 cGy	68.4 cGy